nature cell biology

Synthetic hydrogels for human intestinal organoid generation and colonic wound repair

Ricardo Cruz-Acuña[1,2,9], Miguel Quirós[3,9], Attila E. Farkas[4], Priya H. Dedhia[5,6,7], Sha Huang[5,6,7], Dorothée Siuda[3], Vicky García-Hernández[3], Alyssa J. Miller[5], Jason R. Spence[5,6,7,10], Asma Nusrat[3,10] and Andrés J. García[2,8,10]

In vitro **differentiation of human intestinal organoids (HIOs) from pluripotent stem cells is an unparalleled system for creating complex, multicellular three-dimensional structures capable of giving rise to tissue analogous to native human tissue. Current methods for generating HIOs rely on growth in an undefined tumour-derived extracellular matrix (ECM), which severely limits the use of organoid technologies for regenerative and translational medicine. Here, we developed a fully defined, synthetic hydrogel based on a four-armed, maleimide-terminated poly(ethylene glycol) macromer that supports robust and highly reproducible *in vitro* growth and expansion of HIOs, such that three-dimensional structures are never embedded in tumour-derived ECM. We also demonstrate that the hydrogel serves as an injection vehicle that can be delivered into injured intestinal mucosa resulting in HIO engraftment and improved colonic wound repair. Together, these studies show proof-of-concept that HIOs may be used therapeutically to treat intestinal injury.**

Human pluripotent stem cells (hPSCs), such as embryonic stem cells (ESCs)[1] and induced pluripotent stem cells (iPSCs)[2], are important cell sources for regenerative therapies and modelling of human diseases[3–5]. *In vitro* generation of human organoids from hPSCs offers unparalleled strategies for generating multicellular three-dimensional 3D structures recapitulating important features of epithelial and mesenchymal tissues[6–9]. For example, human intestinal organoid (HIO) technology provides a powerful platform for functional modelling and repair of genetic defects in human intestinal development[10,11] and the establishment of chronic disease models, such as inflammatory bowel disease[12].

To generate HIOs, hPSCs are cultured and differentiated using growth factors in a Matrigel-coated substrate, giving rise to 3D intestinal spheroids that are collected and encapsulated within Matrigel for expansion into HIOs[13]. Matrigel is a heterogeneous, complex mixture of ECM proteins, proteoglycans and growth factors secreted by Engelbreth–Holm–Swarm mouse sarcoma cells[14], which is required for 3D growth and expansion of HIOs. However, Matrigel suffers from lot-to-lot compositional and structural variability and, importantly, this tumour-derived matrix has limited clinical translational potential[15]. Indeed, a synthetic alternative to Matrigel that supports murine intestinal stem cell expansion and organoid formation has recently been reported[15].

Here, we describe a completely synthetic hydrogel that supports *in vitro* generation of intestinal organoids from human ESC- and iPSC-derived 3D spheroids without Matrigel encapsulation and promotes their engraftment and healing of murine colonic mucosal wounds. Hydrogel mechanical properties and adhesive ligand type were key parameters in engineering a synthetic ECM mimic that supported HIO viability, expansion and development. In addition, this synthetic hydrogel served as an injectable vehicle to deliver HIOs to intestinal wounds via a colonoscope resulting in organoid survival, engraftment and wound repair. The modular design of this synthetic matrix and the ability to deliver it via endoscopic techniques support the translational potential of this delivery platform for regenerative medicine and overcomes limitations associated with the use of Matrigel for hPSC-based organoid technologies.

Engineered hydrogels support HIO viability

We selected a hydrogel platform based on a four-arm poly(ethylene glycol) (PEG) macromer with maleimide groups at each terminus (PEG-4MAL) (Supplementary Fig. 1a), which exhibits high

[1]Wallace H. Coulter Department of Biomedical Engineering, Georgia Institute of Technology, Atlanta, Georgia 30332, USA. [2]Parker H. Petit Institute for Bioengineering and Biosciences, Georgia Institute of Technology, Atlanta, Georgia 30332, USA. [3]Department of Pathology, University of Michigan, Ann Arbor, Michigan 48104, USA. [4]Institute of Biophysics, Biological Research Centre, Hungarian Academy of Sciences, Szeged 6726, Hungary. [5]Department of Internal Medicine, Division of Gastroenterology, University of Michigan Medical School, Ann Arbor, Michigan 48104, USA. [6]Department of Cell and Developmental Biology, University of Michigan Medical School, Ann Arbor, Michigan 48104, USA. [7]Center for Organogenesis, University of Michigan Medical School, Ann Arbor, Michigan 48104, USA. [8]George W. Woodruff School of Mechanical Engineering, Georgia Institute of Technology, Atlanta, Georgia 30332, USA. [9]These authors contributed equally to this work. [10]Correspondence should be addressed to J.R.S., A.N. or A.J.G. (e-mail: spencejr@umich.edu or anusrat@med.umich.edu or andres.garcia@me.gatech.edu)

Received 28 March 2017; accepted 19 September 2017; published online 23 October 2017; DOI: 10.1038/ncb3632

cytocompatibility and minimal toxicity and inflammation *in vivo*[16,17]. Moreover, this hydrogel system offers significant advantages due to its well-defined structure, stoichiometric incorporation of biofunctional groups, and tunable reaction timescales for *in situ* gelation for *in vivo* applications[16,17].

PEG-4MAL macromers were functionalized with adhesive peptides and crosslinked in the presence of cells to generate PEG-4MAL hydrogels (Supplementary Fig. 1a,b). The mechanical properties of the hydrogel were tuned by varying polymer density (Supplementary Fig. 1c,d). We explored hydrogel formulations that supported the viability of ESC-derived HIOs that were first generated in Matrigel. After HIOs were grown in Matrigel, they were retrieved and encapsulated in PEG-4MAL hydrogel formulations (Supplementary Fig. 1e). As ECM mechanical properties influence epithelial cell behaviours[18], we investigated the influence of hydrogel polymer density (3.5–6.0% wt/vol), which controls hydrogel mechanical properties (Supplementary Fig. 1c,d), on HIO viability at day 7 post-encapsulation (Fig. 1a). For reference, the mechanical properties of Matrigel ($G' = 78$ Pa, $G'' = 5.8$ Pa) are in the range of the 3.5–4.0% PEG-4MAL formulations. These synthetic hydrogels were engineered to present a constant 2.0 mM RGD adhesive peptide (GRGDSPC) density and crosslinked with the protease-degradable peptide GPQ-W (GCRDGPQGIWGQDRCG). This adhesive peptide type and density were chosen as they have been shown to support epithelial cell viability and cyst formation in PEG-4MAL hydrogels[18]. The protease-degradable crosslinking peptide is necessary for cell-dependent matrix remodelling, cell migration and growth[18,19]. HIOs embedded in 3.5% and 4.0% PEG-4MAL gels grew as cysts with an epithelium and central lumen, and maintained high viability for at least seven days in culture comparable with growth and viability of HIOs in Matrigel (Fig. 1a). Quantification of organoid viability area demonstrated no significant differences between HIOs embedded in 3.5% or 4.0% PEG-4MAL gels and HIOs in Matrigel (Fig. 1b). In contrast, organoids encapsulated in 5.0% or 6.0% PEG-4MAL hydrogels exhibited significantly reduced viability at day 7 after encapsulation as compared with HIOs embedded in 3.5%, 4.0% PEG-4MAL gels or Matrigel (Fig. 1a,b). These results suggest polymer density-dependent effects on HIO survival within PEG-4MAL hydrogels. Although 3.5% PEG-4MAL hydrogels supported high HIO viability, this formulation was less mechanically stable compared with 4.0% PEG-4MAL hydrogels by seven days in culture. We therefore selected 4.0% PEG-MAL hydrogels for subsequent studies.

Interactions between adhesion receptors and ECM provide signals critical for cell survival, proliferation and differentiation[20]. Therefore, we examined whether the adhesive ligand type in the synthetic hydrogel affects HIO viability. Organoids were embedded within PEG-4MAL formulations of 4.0% polymer density and constant GPQ-W crosslinking peptide density but with different cysteine-terminated adhesive peptides (all at 2.0 mM; Fig. 1c,d): RGD, laminin α1 chain-derived AG73 (CGGRKRLQVQLSIRT)[21], type I collagen-mimetic triple helical GFOGER (GYGGGP(GPP)$_5$GFOGER(GPP)$_5$GPC)[22], and laminin α1 chain-derived IKVAV (CGGAASIKVAVSADR)[23]. As the adhesive peptide-functionalized macromer building blocks of the hydrogel are symmetric and form a regular mesh structure that is fully swollen, the adhesive peptide is uniformly distributed throughout the hydrogel network within the 'statistical average' of the mesh size (30–40 nm). Furthermore, because of the small size of the PEG macromer arms and the swollen state of the gel, the mobility of the adhesive peptide is very limited and there is no effective clustering of the adhesive peptide[18]. Nevertheless, changes in adhesive peptide density at the nanoscale cannot be completely ruled out. Organoids encapsulated in RGD-functionalized hydrogels maintained high viability for at least seven days after encapsulation (Fig. 1c,d and Fig. 2a), similar to viability within Matrigel. In contrast, organoids encapsulated in PEG-4MAL hydrogels functionalized with AG73, GFOGER or IKVAV showed reduced viability at seven days post-encapsulation (Fig. 1c,d). Adhesion to RGD was required for HIO viability, as organoids encapsulated in hydrogels presenting an inactive scrambled peptide (RDG) showed reduced viability at seven days post-encapsulation (Fig. 2b). Finally, organoids exhibited low viability at seven days post-encapsulation in hydrogels crosslinked with non-degradable molecules (dithiothreitol (DTT), Fig. 2c), demonstrating that prolonged survival of HIO requires a degradable matrix. Taken together, these results identify an engineered hydrogel formulation (4.0% polymer density, 2.0 mM RGD adhesive peptide, GPQ-W crosslinking peptide) that supports high viability for established HIOs, and which was used for all subsequent experiments.

Engineered hydrogel supports HIO development

We next examined HIO maintenance during culture in engineered hydrogels. Over several days in culture, established HIOs grew in size, changed shape, maintained a central lumen, and displayed epithelial budding at the interface with the hydrogel (Fig. 2d). In addition, mesenchymal cells were observed migrating into the hydrogel, similar to HIOs maintained in Matrigel (Fig. 2d,e). To further characterize the intestinal epithelium of HIOs, we examined cell proliferation and apicobasal polarity in HIOs generated in Matrigel and those transferred to the engineered PEG-4MAL hydrogels. After seven days in culture, HIOs stained positive for Ki-67, indicating cell proliferation, demonstrated appropriate polarization of apical (ezrin) and basolateral (β-catenin) proteins, and localization of an epithelial tight junction protein (ZO-1) (ref. 24) (Fig. 2f,g). The staining patterns were similar when comparing HIOs maintained in PEG-4MAL hydrogel and Matrigel (Fig. 2f,g), demonstrating that the engineered PEG-4MAL hydrogel robustly supports HIO maintenance.

Engineered hydrogel generates HIOs from spheroids

The use of Matrigel to generate HIOs is a fundamental roadblock to the clinical translation of organoid technologies. We therefore examined whether the engineered PEG-4MAL hydrogel supports survival of hESC-derived intestinal spheroids and growth into HIOs without ever embedding in Matrigel. After four to five days of induction towards the intestinal lineage on a Matrigel-coated substrate, small 3D intestinal spheroids self-assemble and bud off from the cultured monolayer losing contact with Matrigel. Detached, floating mCherry-expressing intestinal spheroids were collected from the media and encapsulated in PEG-4MAL hydrogels formulated over a range of polymer densities (3.5–12.0%) (Supplementary Fig. 1f) to examine a range of mechanical properties (Supplementary Fig. 1c,d). All of these hydrogels were engineered to present 2.0 mM RGD adhesive peptide and crosslinked with GPQ-W. Spheroids embedded in 3.5%

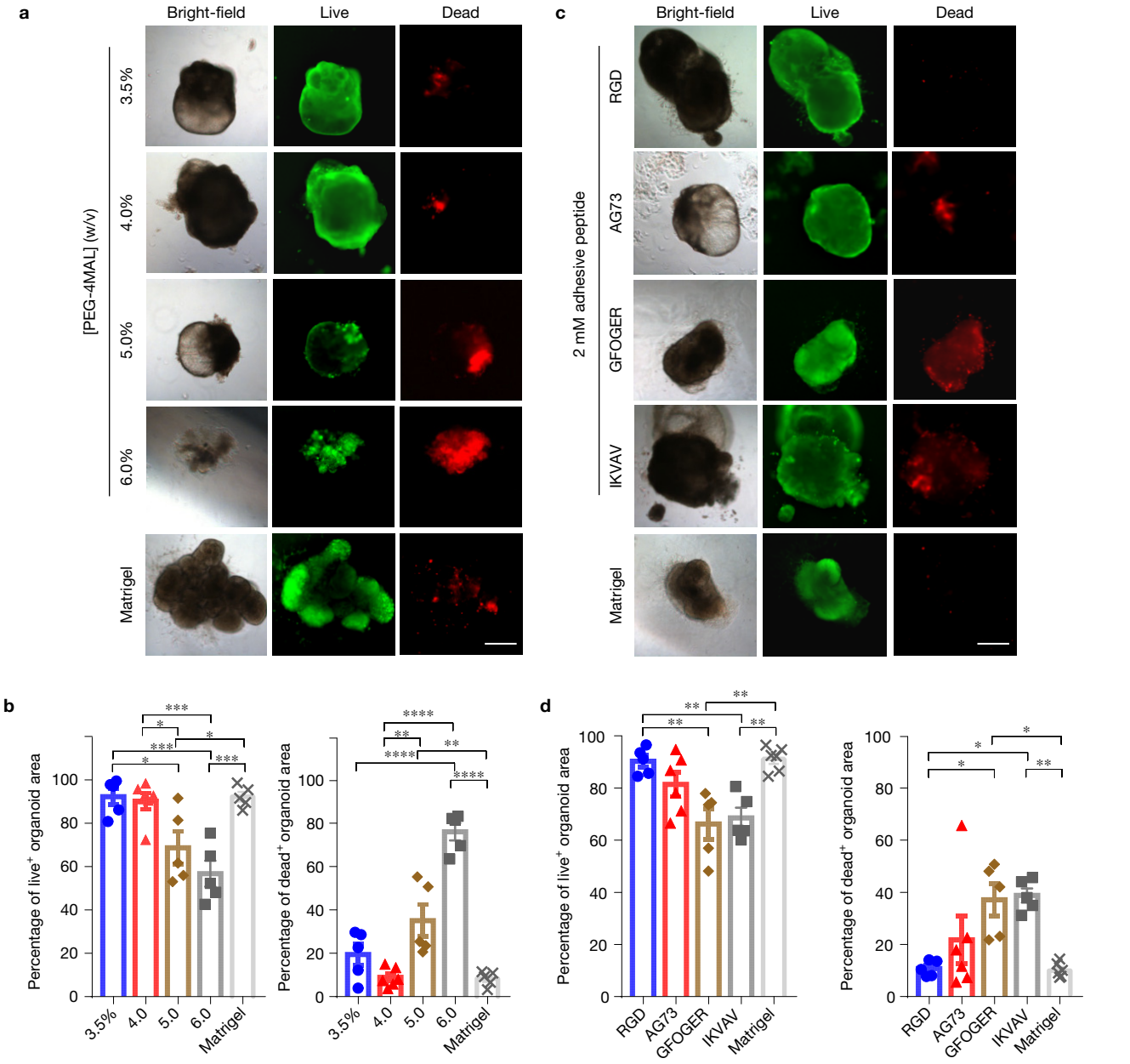

Figure 1 PEG-4MAL polymer density and adhesive ligand type control HIO viability. (**a**) Transmitted light and fluorescence microscopy images of HIOs cultured in PEG-4MAL hydrogels of different polymer density or Matrigel. HIO viability was assessed at seven days after encapsulation. Scale bar, 500 μm. (**b**) Percentage of total organoid area stained for live or dead (mean ± s.e.m.) after seven days of encapsulation ($n = 5$ organoids analysed for all groups, except $n = 6$ organoids analysed for the 4.0% group). (**c**) Transmitted light and fluorescence microscopy images of HIOs cultured in 4.0% PEG-4MAL hydrogels functionalized with different adhesive peptides or Matrigel. HIO viability was assessed at seven days after encapsulation. Scale bar, 500 μm. (**d**) Percentage of total organoid area stained for live or dead (mean ± s.e.m.) after 7 days of encapsulation ($n = 5$ organoids analysed for all groups, except $n = 6$ organoids analysed for AG73 and Matrigel groups). For **b**,**d**, one-way ANOVA with Tukey's multiple comparisons test showed significant differences between 4.0% PEG-4MAL or Matrigel and 5.0 or 6.0% PEG-4MAL (**b**), and between PEG-4MAL-RGD or Matrigel and PEG-4MAL-GFOGER or -IKVAV (**d**). ($^{*}P < 0.05$, $^{**}P < 0.01$, $^{***}P < 0.001$, $^{****}P < 0.0001$.) In **a**–**d**, three independent experiments were performed and data are presented for one of the experiments. Every independent experiment was performed with six gel samples per experimental group (PEG-4MAL, Matrigel). Source data are available in Supplementary Table 1.

and 4.0% PEG-4MAL maintained viability at 2 h after encapsulation and grew into larger structures reminiscent of organoids with high viability at five days after encapsulation (Fig. 3a). In contrast, spheroids encapsulated in 8.0% and 12.0% PEG-4MAL hydrogels displayed significantly lower viability at 2 h post-encapsulation when compared with spheroids embedded in 3.5% or 4.0% PEG-4MAL (Fig. 3a). Consistent results were observed between hESC- and hiPSC-derived spheroids (Supplementary Fig. 2). hiPSC-derived intestinal spheroids encapsulated in 4.0% PEG-4MAL grew into organoids with high viability at five days after encapsulation and developed over three

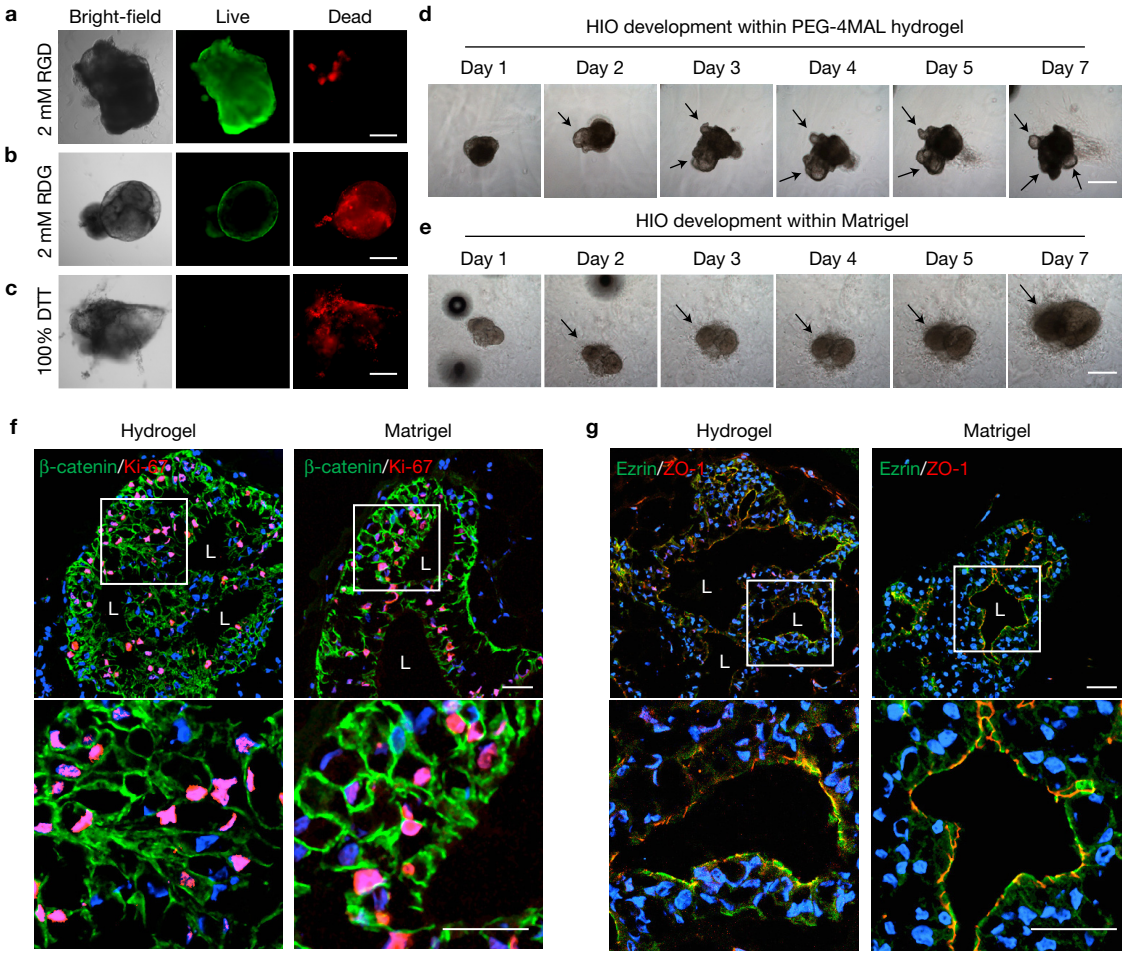

Figure 2 Engineered PEG-4MAL supports HIO development. (**a**–**c**) Transmitted light and fluorescence microscopy images of HIOs cultured in 4.0% PEG-4MAL hydrogels functionalized with RGD (**a**), inactive, scrambled RDG peptide (**b**) or non-degradable crosslinker (DTT) (**c**). HIO viability was assessed at seven days after encapsulation. Scale bars, 500 μm. (**d**,**e**) Transmitted light microscopy images of Matrigel-generated HIOs cultured within 4.0% PEG-4MAL-RGD hydrogel (**d**) or Matrigel (**e**) over time. The black arrows show epithelial budding. Scale bars, 500 μm. (**f**,**g**) Fluorescence microscopy images of a HIO at seven days after encapsulation in 4.0% PEG-4MAL-RGD hydrogel or Matrigel, and labelled for β-catenin, proliferative cells (Ki-67) (**f**), and epithelial apical polarity (ezrin) and tight junctions (ZO-1) (**g**). DAPI, counterstain. 'L' indicates HIO lumen. Scale bars, 100 μm. In **a**–**g**, three independent experiments were performed and data are presented for one of the experiments. Every experiment was performed with four (**a**–**c**), six (**f**,**g**) or twelve (**d**,**e**) gel samples per experimental group (PEG-4MAL, Matrigel).

weeks into HIOs similar to spheroids encapsulated in Matrigel (Supplementary Fig. 2a,b). In contrast, hiPSC-derived spheroids encapsulated in 8.0% PEG-4MAL hydrogels showed very low viability by one day post-encapsulation (Supplementary Fig. 2c).

The strong dependence of spheroid and HIO viability on hydrogel polymer density suggests that the mechanical properties of these synthetic matrices regulate organoid survival. However, varying polymer density also alters the mesh size for these networks, which can impact diffusional properties of the hydrogel. It is not possible to uncouple mechanical properties from diffusional properties over the full range of polymer densities (3.5–12.0%) examined in this study. However, we compared organoid viability and size in RGD-functionalized hydrogels from different macromer sizes (relative molecular mass of 20,000 versus 40,000) but different polymer densities (4.0% versus 8.0%) and engineered to have equivalent crosslinking densities (Supplementary Fig. 3a–c). These hydrogels exhibit different diffusive characteristics/permeability caused by the differences in macromer arm length but have equivalent mechanical properties due to equivalent crosslinking densities[18]. ESC-derived spheroids developed normally into HIOs after five days of encapsulation in either hydrogel formulation showing no differences in HIO viability (Supplementary Fig. 3a,b), and no differences in projected area and longest distance between two points along the projected area (Feret diameter; Supplementary Fig. 3c). These results suggest that polymer density-dependent spheroid survival and development into HIOs is related to hydrogel mechanical properties. Furthermore, we evaluated the role of known mechanotransduction pathways on spheroid survival. Inhibition of nuclear translocation of yes-associated protein (YAP), which has been implicated in mechanotransduction and regulation of intestinal stem cell self-renewal[15], using verteporfin resulted in significant cell death for spheroids encapsulated in PEG-4MAL hydrogels compared with vehicle control (Supplementary Fig. 3d–f). Treatment with blebbistatin or Y-27632, which inhibit myosin II

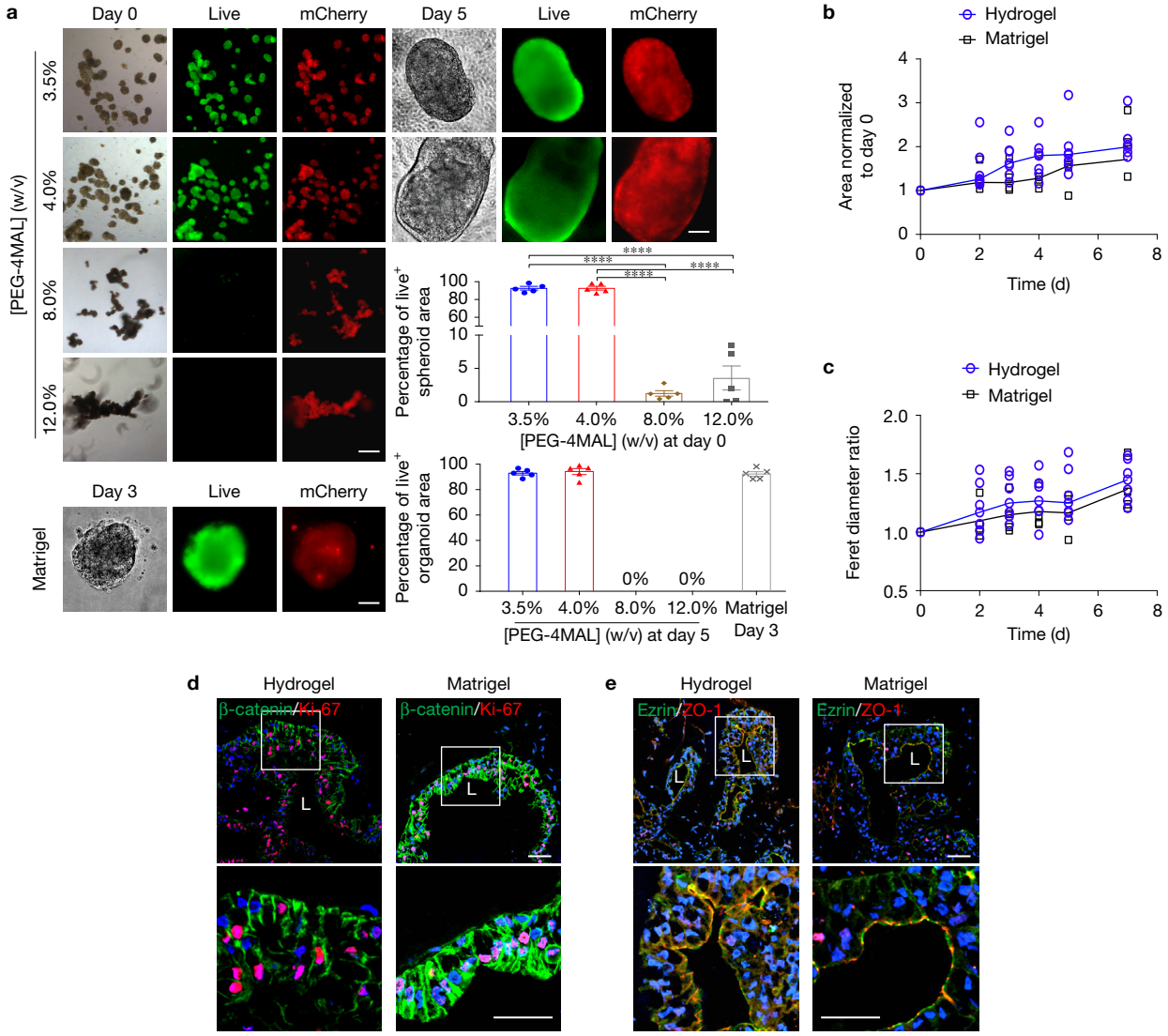

Figure 3 PEG-4MAL polymer density regulates HIO generation from intestinal spheroids in the absence of Matrigel embedding. (**a**) Transmitted light and fluorescence microscopy images of mCherry-spheroids cultured in PEG-4MAL hydrogels of different polymer density or Matrigel. Spheroids viability was assessed by Calcein-AM labelling at 2 h after encapsulation (day 0) and at day 5 for PEG-4MAL conditions, and at day 3 for Matrigel. Scale bars, 100 μm. Viability is quantified as the percentage of total spheroid or organoid area stained for live or dead (mean ± s.e.m.; $n = 5$ organoids analysed per condition per time point). One-way ANOVA with Tukey's multiple comparisons test showed significant differences between 3.5% or 4.0% PEG-4MAL and 8.0% or 12.0% PEG-4MAL at day 0 (**** $P < 0.0001$). (**b**,**c**) HIO projected area (**b**) and Feret diameter normalized to day 0 values (**c**) at different time points after encapsulation in 4.0% PEG-4MAL-RGD hydrogel (filled blue circle) or Matrigel (black square) ($n = 6$ organoids for PEG-4MAL and $n = 4$ organoids for Matrigel per time point). Repeated measures two-way ANOVA showed no significant difference between matrix types ($P > 0.05$). The line represents the mean of the individual data points at each time point. (**d**,**e**) Fluorescence microscopy images of a HIO at 21 days after encapsulation in 4.0% PEG-4MAL-RGD hydrogel or Matrigel and labelled for β-catenin, proliferative cells (Ki-67) (**d**), and epithelial apical polarity (ezrin) and tight junctions (ZO-1) (**e**). DAPI, counterstain. 'L' indicates HIO lumen. Scale bars, 100 μm. Three independent experiments were performed and data are presented for one of the experiments. Every experiment was performed with six gel samples per experimental group (PEG-4MAL, Matrigel). Source data are available in Supplementary Table 1.

and Rho-associated kinase[25,26], respectively, resulted in dose-dependent increases in apoptosis and spheroid death at one day post-encapsulation (Supplementary Fig. 3d–f). These results provide a preliminary indication that YAP and cellular contractility are important in the initial stages of human intestinal spheroid survival and development into HIOs.

We next analysed HIO generation from ESC-derived spheroids cultured within the engineered synthetic matrix (4.0% polymer density, 2.0 mM RGD, GPQ-W crosslinker). Intestinal spheroids cultured within PEG-4MAL hydrogels grew in size over seven days as shown by a twofold increase in projected area (Fig. 3b) and a 1.4-fold increase in Feret diameter (Fig. 3c) as compared with the day of encapsulation (day 0; Fig. 3b,c). There were no differences in spheroid area, diameter or growth rates between spheroids cultured in PEG-4MAL hydrogels and Matrigel (Fig. 3b,c). As we observed for established HIOs, spheroids changed shape during

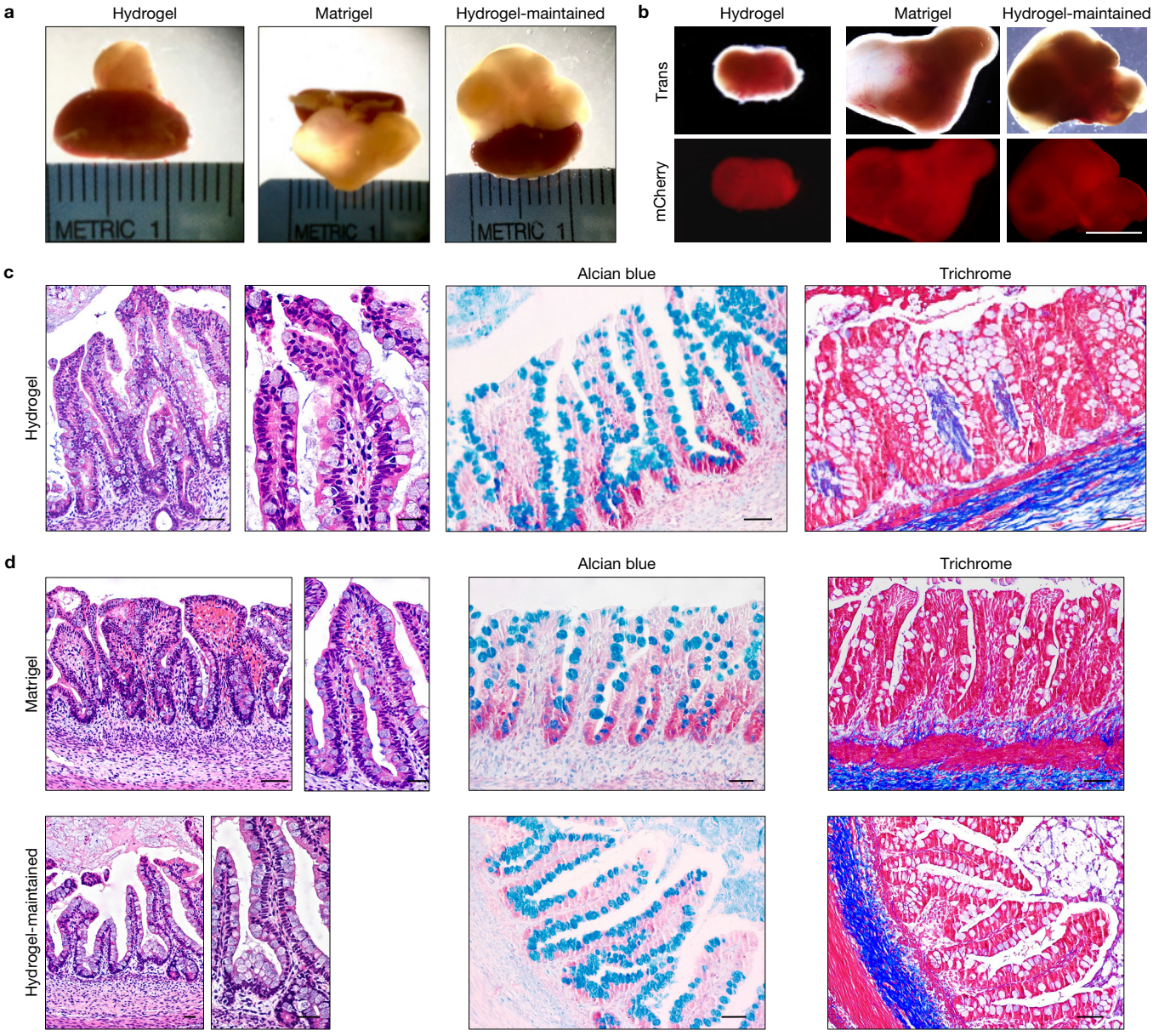

Figure 4 PEG-4MAL-generated HIOs develop a mature intestinal tissue structure *in vivo*. (**a**) Micrographs of dissected kidneys containing HIOs generated within PEG-4MAL hydrogel or Matrigel, or generated within Matrigel and maintained within PEG-4MAL (hydrogel-maintained). (**b**) Transmitted light and fluorescence microscopy (mCherry) images of harvested organoids. Scale bar, 0.5 cm. (**c**,**d**) Haematoxylin and eosin staining demonstrates the mature human intestinal crypt–villus structure, and alcian blue and trichrome staining reveal the presence of differentiated goblet cells and organized collagen fibres. Scale bars, 100 μm. One experiment was performed using three mice per experimental group.

expansion and displayed epithelial budding at the interface with the hydrogel and cell outgrowths migrating into the hydrogel (Supplementary Fig. 2d). During HIO development, spheroids cultured in PEG-4MAL hydrogels were passaged in a similar manner as previously described for Matrigel[13,27]. Immunostaining analyses at 21 days post-encapsulation demonstrated that organoids generated in engineered PEG-4MAL hydrogels were proliferating as shown by Ki-67 labelling, had polarized distribution of apical ezrin and basolateral β-catenin, and expressed ZO-1 in the apical junctional complex (Fig. 3d,e). These staining patterns were identical to organoids generated in Matrigel. Quantitative polymerase chain reaction with reverse transcription (RT–qPCR) confirmed that expression levels of pluripotency (OCT4), endoderm (FOXA2), and epithelial junction (ZO1, ECAD and CLDN2) markers in hydrogel-encapsulated spheroids were comparable to those embedded in Matrigel and had similar behaviours during early time points while developing into HIOs (Supplementary Fig. 4). Finally, to test whether these synthetic matrices are suitable for the culture of other human organoids, we embedded human lung organoids (HLOs)[28,29] in engineered PEG-4MAL hydrogels (Supplementary Fig. 5). HLOs cultured in PEG-4MAL hydrogels maintained high viability seven days after encapsulation (Supplementary Fig. 5a), and demonstrated

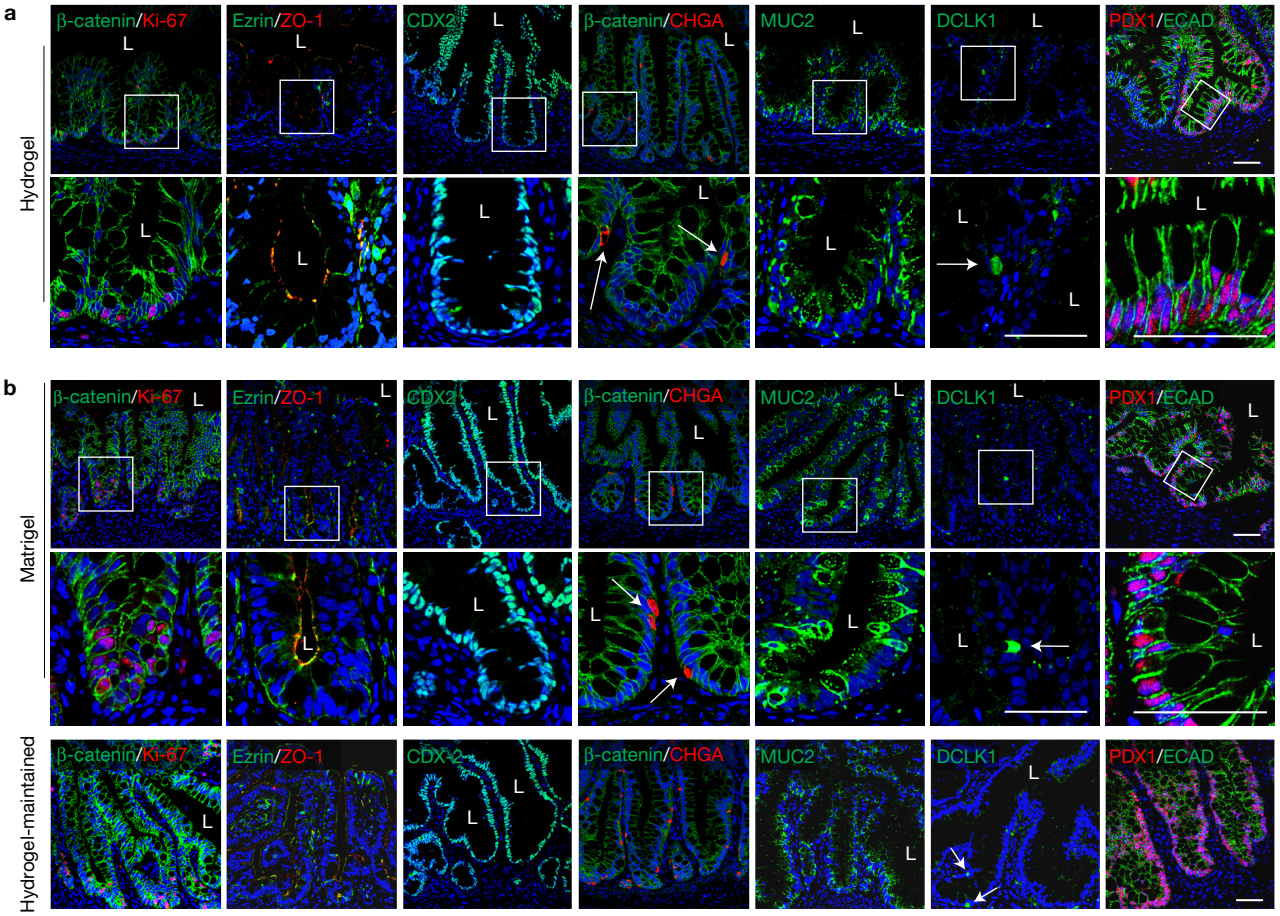

Figure 5 PEG-4MAL-generated HIOs differentiate into mature intestinal tissue *in vivo*. (**a**,**b**) Fluorescence microscopy images of HIOs generated within PEG-4MAL hydrogel (**a**) or Matrigel, or generated within Matrigel and maintained within PEG-4MAL (hydrogel-maintained) (**b**), and labelled for β-catenin, proliferative cells (Ki-67), epithelial apical polarity (ezrin) and junctions (ZO-1 and ECAD), intestinal epithelial protein CDX2, enteroendocrine cells (CHGA), goblet cells (MUC2), tuft cells (DCLK1) and small intestinal marker (duodenum; PDX1). DAPI, counterstain. 'L' indicates HIO lumen. The white arrows show enteroendocrine cells or tuft cells. Scale bars, 50 μm. One experiment was performed using three mice per experimental group.

an organized lung epithelium (ECAD), lumen formation, and specific markers for lung epithelium (NKX2.1) and airway basal cells (P63) as assessed by immunostaining analyses (Supplementary Fig. 5b)[28,29]. Taken together, these results demonstrate that this fully synthetic hydrogel supports the generation of ESC- and iPSC-derived HIOs from the intestinal spheroid stage without the use of Matrigel, and has the potential to be adapted for the generation of different human organoids.

Hydrogel-generated HIOs differentiate *in vivo*

We next examined the potential of hydrogel-grown HIOs to differentiate into mature intestinal tissue *in vivo* as previously demonstrated[24,30]. mCherry-expressing spheroids that were embedded and grown within engineered PEG-4MAL hydrogels or in Matrigel for three weeks were recovered from their respective matrix and implanted under the kidney capsule of immunocompromised NSG mice (Fig. 4). In addition, HIOs grown in Matrigel for two weeks and then transferred and cultured within PEG-4MAL hydrogels for one week (hydrogel-maintained) were implanted under the kidney capsule (Fig. 4a,b,d). After 12 weeks, implanted kidneys contained mCherry-expressing HIOs that were 10- to 40-fold larger in area than at the time of implantation (Fig. 4a,b), consistent with previous reports. Dissected PEG-4MAL-generated HIOs showed differentiated intestinal epithelium that resembled mature human intestine with crypt–villus architecture and underlying lamina propria, muscularis mucosae and submucosa[24], with structured collagen fibres (trichrome) and presence of differentiated goblet cells (alcian blue), comparable to Matrigel-generated and hydrogel-maintained organoids (Fig. 4c,d). Polarized epithelial differentiation of PEG-4MAL hydrogel-generated HIOs was demonstrated by immunostaining for β-catenin, ezrin, ZO-1 and ECAD (Fig. 5a). Additionally, PEG-4MAL-generated organoid epithelium showed localized cell proliferation (Ki-67) at the base of the crypt where the intestinal stem cells reside, and expressed characteristic markers for the intestinal epithelial protein CDX2, enteroendocrine cells (CHGA), goblet cells (MUC2) and tuft cells (DCLK1) (ref. 31). Furthermore, PEG-4MAL-generated HIOs expressed PDX1, demonstrating a duodenum regional identity (Fig. 5a)[13]. Expression was comparable to Matrigel-generated organoids and hydrogel-maintained organoids (Fig. 5b). These results demonstrate that HIOs generated in the engineered synthetic

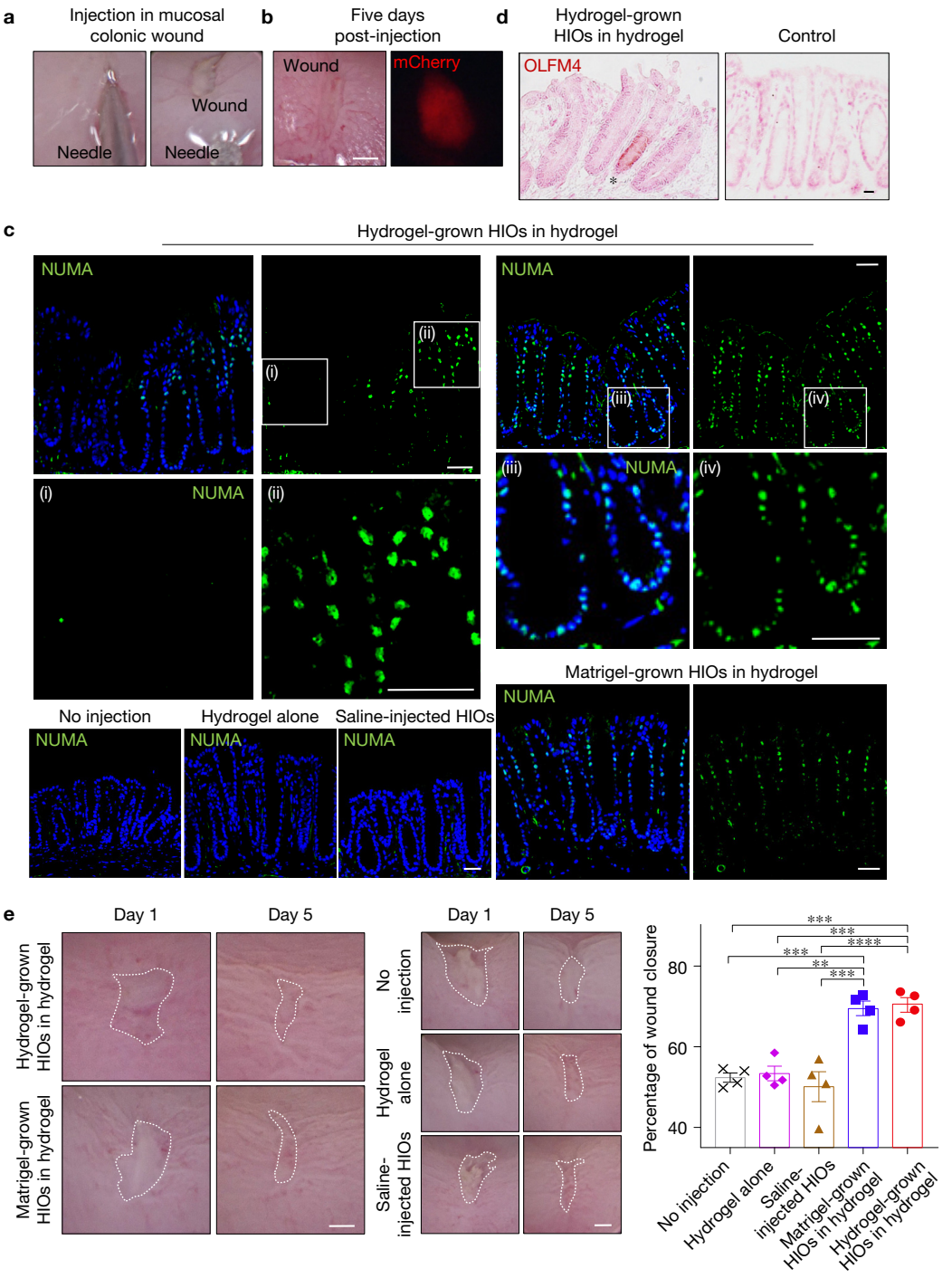

Figure 6 PEG-4MAL serves as an injectable delivery vehicle to promote HIO engraftment and wound closure. (**a**) PEG-4MAL-generated HIOs mixed with engineered hydrogel precursor solutions were injected underneath mechanically induced mucosal wounds, as seen through the colonoscope camera. (**b**) Mechanically induced mucosal wound and fluorescence imaging (mCherry) at the wound site at 5 days post-injection. Scale bar, 500 μm. (**c**) Fluorescence microscopy images of murine colonic tissue at the wound site labelled for human cell nuclei (NUMA) at four weeks post-delivery. Left: images from the wound edge showing insets from adjacent host tissue (i) and the wound (ii). Right: images from the wound centre showing insets at the wound site. DAPI, counterstain. Scale bars, 100 μm. (**d**) *In situ* hybridization, staining for human OLFM4^{+} cells. Scale bar, 50 μm. (**e**) Images of mucosal wounds at 1 day (prior to injection) or 5 day post-injury in murine colon as seen through the colonoscope camera. Mucosal wound area at 5 days post-injury was normalized to day 1 (prior to injection) values (mean ± s.e.m.). Five colonic wounds per mouse were analysed and averaged ($n=4$ mice per condition). One-way ANOVA with Tukey's multiple comparisons test showed significant difference between hydrogel-grown HIOs in hydrogel (filled red circles) or Matrigel-grown HIOs in hydrogel (filled blue squares) and saline-injected HIOs (filled brown triangles), hydrogel alone (filled purple lozenges), or no injection group (black crosses) ($^{**}P<0.01$, $^{***}P<0.001$, $^{****}P<0.0001$). Scale bars, 500 μm. Two independent experiments were performed and data are presented for one of the experiments. Experiments performed with four mice per experimental group (five colonic wounds/injections per mouse; **a**–**e**). Source data are available in Supplementary Table 1.

matrix can differentiate into mature intestinal tissue in an *in vivo* environment to the same extent as HIOs generated within Matrigel. These findings establish engineered synthetic PEG-4MAL hydrogels as a robust alternative to Matrigel with significant implications for translational medicine.

Hydrogels as a HIO delivery vehicle to heal colonic wounds

A key advantage of the PEG-4MAL hydrogel system is control over gelling time, so that the hydrogel components can be injected as a solution that gels *in situ*[17]. We therefore explored the use of the engineered hydrogel as a delivery vehicle for HIOs into murine intestinal mucosal wounds using a murine colonoscope. HIOs generated in PEG-4MAL hydrogels or Matrigel were recovered from their matrix, mixed with the hydrogel precursor solution, and injected at the site of mechanically induced mucosal wounds in the distal colon of immunocompromised mice (Fig. 6a and Supplementary Fig. 6a)[32]. Wound closure was evaluated using a colonoscope, and fluorescence imaging showed localized expression of mCherry-positive tissue at the wound site five days post-injection (Fig. 6b). Immunostaining at four weeks post-injection demonstrated that HIO delivery via the synthetic hydrogel resulted in HIO engraftment into host intestinal epithelial tissue as shown by positive staining for human nuclei (NUMA) to detect HIOs generated in either the PEG-4MAL hydrogel or Matrigel (Fig. 6c). Importantly, no staining was evident for no-injection control, hydrogel alone and HIOs injected in saline (Fig. 6c), demonstrating that the hydrogel delivery vehicle is required for HIO engraftment and wound repair. Examination of HIO engraftment at the wound edge demonstrated staining for human cells adjacent to host tissue that stained negative for human markers. Engraftment of human cells into the colonic wound was also confirmed by positive staining for human mitochondria (HUMIT; Supplementary Fig. 6b). Furthermore, colonic wounds treated with HIOs delivered with hydrogel showed positive staining for an *OLFM4* probe specific to human cells at the base of the crypt-like domain (Fig. 6d and Supplementary Fig. 6c), a pattern consistent with staining in the normal adult human colon (Supplementary Fig. 6c), which is also consistent with previous reports of human OLFM4 protein and/or messenger RNA localization[33–35]. In addition, several negatively stained human crypt-like domains were adjacent to mouse intestinal crypts that stained positive for a mouse-specific *Lgr5* probe (Supplementary Fig. 6d) via *in situ* hybridization[36]. These observations were compared with control tissue sections from immunocompromised mice that did not undergo colonic injuries or received HIO injections (Fig. 6d and Supplementary Fig. 6d).

We also examined whether delivered HIOs promote colonic mucosal wound repair (Fig. 6e). Strikingly, delivery of HIOs to colonic wounds using the hydrogel carrier significantly increased wound closure compared with untreated wounds and wounds treated with hydrogel alone or HIOs without the hydrogel carrier (Fig. 6e). No differences were observed in wound closure between HIOs generated in the synthetic hydrogels and Matrigel. Taken together, these results demonstrate that the engineered PEG-4MAL hydrogel serves as an injectable delivery vehicle that supports localized HIO engraftment in colonic mucosal wounds and enhances wound closure. These findings establish the clinical translational potential of the synthetic hydrogel as an *in vivo* delivery vehicle for hPSC-derived HIOs and provide proof-of-concept that HIOs may be used therapeutically to treat intestinal injury or disease.

In this study, we engineered a completely synthetic hydrogel that supports *in vitro* generation of intestinal organoids from hPSC-derived spheroids without the need of Matrigel encapsulation. Both mechanical and biochemical properties of the synthetic ECM were important to intestinal organoid formation, and we identified an optimal formulation that supports intestinal spheroid survival, expansion and epithelial differentiation into HIOs and differentiation into mature intestinal tissue *in vivo* to similar levels as Matrigel. In addition, we showed that this synthetic matrix supports the development of other human organoids such as HLOs. The requirement for specific mechanical and cell adhesive properties in the synthetic matrix is consistent with previous work showing that epithelial cell cyst growth, polarization and lumen formation are restricted to a narrow range of ECM elasticity and that adhesive peptide type regulates apicobasal polarity and lumenogenesis during epithelial morphogenesis in 3D cultures[18]. Interestingly, the mechanical properties and protease degradation characteristics that supported hPSC-derived organoids in this study are different from those recently identified for murine *Lrg5*$^{+}$ intestinal stem cell growth and organoid formation[15], which involved more complex, mechanically dynamic properties, and suggest differences between these two organoid sources. This fully synthetic matrix addresses major limitations of Matrigel associated with lot-to-lot compositional and structural variability and its tumour-derived nature that severely restrict scale-up applications and clinical translation.

We also established the use of the engineered hydrogel as a delivery vehicle for HIOs to murine intestinal mucosal wounds using a murine colonoscope. Although other studies have focused on the delivery of murine intestinal organoids into the colonic lumen as a suspension[7], we showed that absence of a delivery vehicle reduces HIO engraftment at the implantation site. Injection of hydrogel liquid precursors and HIOs to mucosal wounds resulted in an *in situ* polymerized hydrogel that supported localized organoid engraftment and enhanced wound repair. Therefore, this delivery strategy forms a basis for the development of HIO-based therapies to treat gastrointestinal diseases in humans involving intestinal epithelial wounds (for example, inflammatory bowel disease). Furthermore, the modular nature of this hydrogel platform allows for the adaptation to *in vitro* generation and *in vivo* delivery of other human PSC-derived organoids (for example, lung) for regenerative medicine. □

METHODS

Methods, including statements of data availability and any associated accession codes and references, are available in the online version of this paper.

Note: Supplementary Information is available in the online version of the paper

ACKNOWLEDGEMENTS

This research was supported by the National Institute of Health (A.J.G. was supported by R01 AR062368 and R01 AR062920; A.N. was supported by DK055679, DK059888 and DK089763) and a seed grant from the Regenerative Engineering and Medicine Research Center between Emory University, Georgia Tech and the University of Georgia. J.R.S. was supported by the Intestinal Stem Cell Consortium (U01DK103141), a collaborative research project funded by the National Institute of Diabetes and Digestive and Kidney Diseases (NIDDK) and the National Institute

of Allergy and Infectious Diseases (NIAID), by the NIAID Novel, Alternative Model Systems for Enteric Diseases (NAMSED) consortium (U19AI116482) and PHS Grant UL1TR000454 from the Clinical and Translational Science Award Program. R.C.-A. is supported by the National Science Foundation Graduate Research Fellowship (DGE-1650044) and the Alfred P. Sloan Foundation's Minority Ph.D. (MPHD) Program (G-2016-20166039). M.Q. is supported by a fellowship from the Crohn's and Colitis Foundation of America (CCFA 326912). A.E.F. is supported by János Bolyai Research Fellowship (BO/00023/17/8). We would like to thank Y.-H. Tsai (University of Michigan, USA) for providing tissue sections for immunohistochemical analysis.

AUTHOR CONTRIBUTIONS

R.C.-A. and M.Q. conducted all experiments, collected data and performed data analyses. A.E.F. assisted with *in vitro* and *in vivo* intestinal crypt experiments. P.H.D. performed the *in vivo* HIO implantation under the kidney capsule experiment. S.H. performed the culture and differentiation of PSCs into intestinal spheroids. D.S. assisted with *in vivo* HIO delivery to mouse colonic wounds. V.G.-H. and A.J.M. performed the *in situ* hybridization experiments. A.N., A.J.G. and J.R.S. conceptualized and designed the project and experiments. R.C.-A., A.J.G., A.N., J.R.S. and M.Q. wrote the manuscript.

COMPETING FINANCIAL INTERESTS

The authors declare no competing financial interests.

Published online at http://dx.doi.org/10.1038/ncb3632
Reprints and permissions information is available online at www.nature.com/reprints
Publisher's note: Springer Nature remains neutral with regard to jurisdictional claims in published maps and institutional affiliations.

1. Thomson, J. A. *et al.* Embryonic stem cell lines derived from human blastocysts. *Science* **282,** 1145–1147 (1998).
2. Takahashi, K. *et al.* Induction of pluripotent stem cells from adult human fibroblasts by defined factors. *Cell* **131,** 861–872 (2007).
3. Takahashi, K. & Yamanaka, S. A developmental framework for induced pluripotency. *Development* **142,** 3274–3285 (2015).
4. Fox, I. J. *et al.* Stem cell therapy. Use of differentiated pluripotent stem cells as replacement therapy for treating disease. *Science* **345,** 1247391 (2014).
5. Robinton, D. A. & Daley, G. Q. The promise of induced pluripotent stem cells in research and therapy. *Nature* **481,** 295–305 (2012).
6. Huch, M. *et al.* Long-term culture of genome-stable bipotent stem cells from adult human liver. *Cell* **160,** 299–312 (2015).
7. Yui, S. *et al.* Functional engraftment of colon epithelium expanded *in vitro* from a single adult Lgr5^{+} stem cell. *Nat. Med.* **18,** 618–623 (2012).
8. Fatehullah, A., Tan, S. H. & Barker, N. Organoids as an *in vitro* model of human development and disease. *Nat. Cell Biol.* **18,** 246–254 (2016).
9. Clevers, H. Modeling development and disease with organoids. *Cell* **165,** 1586–1597 (2016).
10. Dekkers, J. F. *et al.* A functional CFTR assay using primary cystic fibrosis intestinal organoids. *Nat. Med.* **19,** 939–945 (2013).
11. Dekkers, J. F. *et al.* Characterizing responses to CFTR-modulating drugs using rectal organoids derived from subjects with cystic fibrosis. *Sci. Transl. Med.* **8,** 344ra384 (2016).
12. Wells, J. M. & Spence, J. R. How to make an intestine. *Development* **141,** 752–760 (2014).
13. Spence, J. R. *et al.* Directed differentiation of human pluripotent stem cells into intestinal tissue *in vitro*. *Nature* **470,** 105–109 (2011).
14. Hughes, C. S., Postovit, L. M. & Lajoie, G. A. Matrigel: a complex protein mixture required for optimal growth of cell culture. *Proteomics* **10,** 1886–1890 (2010).
15. Gjorevski, N. *et al.* Designer matrices for intestinal stem cell and organoid culture. *Nature* **539,** 560–564 (2016).
16. Phelps, E. A. *et al.* Maleimide cross-linked bioactive PEG hydrogel exhibits improved reaction kinetics and cross-linking for cell encapsulation and *in situ* delivery. *Adv. Mater.* **24,** 64–70 (2012).
17. Phelps, E. A., Headen, D. M., Taylor, W. R., Thule, P. M. & Garcia, A. J. Vasculogenic bio-synthetic hydrogel for enhancement of pancreatic islet engraftment and function in type 1 diabetes. *Biomaterials* **34,** 4602–4611 (2013).
18. Enemchukwu, N. O. *et al.* Synthetic matrices reveal contributions of ECM biophysical and biochemical properties to epithelial morphogenesis. *J. Cell Biol.* **212,** 113–124 (2016).
19. Caiazzo, M. *et al.* Defined three-dimensional microenvironments boost induction of pluripotency. *Nat. Mater.* **15,** 344–352 (2016).
20. Wickström, S. A., Radovanac, K. & Fässler, R. Genetic analyses of integrin signaling. *Cold Spring Harb. Perspect. Biol.* **3,** a005116 (2011).
21. Hoffman, M. P. *et al.* Laminin-1 and laminin-2 G-domain synthetic peptides bind syndecan-1 and are involved in acinar formation of a human submandibular gland cell line. *J. Biol. Chem.* **273,** 28633–28641 (1998).
22. Emsley, J., Knight, C. G., Farndale, R. W. & Barnes, M. J. Structure of the integrin α2β1-binding collagen peptide. *J. Mol. Biol.* **335,** 1019–1028 (2004).
23. Kikkawa, Y. *et al.* Laminin-111-derived peptides and cancer. *Cell Adhes. Migration* **7,** 150–256 (2013).
24. Finkbeiner, S. R. *et al.* Transcriptome-wide analysis reveals hallmarks of human intestine development and maturation *in vitro* and *in vivo*. *Stem Cell Rep.* **4,** 1140–1155 (2015).
25. Straight, A. F. *et al.* Dissecting temporal and spatial control of cytokinesis with a myosin II inhibitor. *Science* **299,** 1743–1747 (2003).
26. Uehata, M. *et al.* Calcium sensitization of smooth muscle mediated by a Rho-associated protein kinase in hypertension. *Nature* **389,** 990–994 (1997).
27. McCracken, K. W., Howell, J. C., Wells, J. M. & Spence, J. R. Generating human intestinal tissue from pluripotent stem cells *in vitro*. *Nat. Protoc.* **6,** 1920–1928 (2011).
28. Dye, B. R. *et al.* A bioengineered niche promotes *in vivo* engraftment and maturation of pluripotent stem cell derived human lung organoids. *eLife* **5,** e19732 (2016).
29. Dye, B. R. *et al.* *In vitro* generation of human pluripotent stem cell derived lung organoids. *eLife* **4,** e05098 (2015).
30. Finkbeiner, S. R. *et al.* Generation of tissue-engineered small intestine using embryonic stem cell-derived human intestinal organoids. *Biol. Open* **4,** 1462–1472 (2015).
31. Gerbe, F., Brulin, B., Makrini, L., Legraverend, C. & Jay, P. DCAMKL-1 expression identifies Tuft cells rather than stem cells in the adult mouse intestinal epithelium. *Gastroenterology* **137,** 2179–2180; author reply 2180–2171 (2009).
32. Leoni, G. *et al.* Annexin A1-containing extracellular vesicles and polymeric nanoparticles promote epithelial wound repair. *J. Clin. Invest.* **125,** 1215–1227 (2015).
33. Jang, B. G. *et al.* Distribution of intestinal stem cell markers in colorectal precancerous lesions. *Histopathology* **68,** 567–577 (2016).
34. Besson, D. *et al.* A quantitative proteomic approach of the different stages of colorectal cancer establishes OLFM4 as a new nonmetastatic tumor marker. *Mol. Cell. Proteom.* **10,** M111.009712 (2011).
35. van der Flier, L. G., Haegebarth, A., Stange, D. E., van de Wetering, M. & Clevers, H. OLFM4 is a robust marker for stem cells in human intestine and marks a subset of colorectal cancer cells. *Gastroenterology* **137,** 15–17 (2009).
36. Barker, N. *et al.* Identification of stem cells in small intestine and colon by marker gene Lgr5. *Nature* **449,** 1003–1007 (2007).

DOI: 10.1038/ncb3632

METHODS

Immunofluorescence analysis. For immunofluorescence labelling of frozen sections from colon, HIOs, kidney capsule implanted-HIOs or HLOs, these were fixed with 3.7% (w/v) paraformaldehyde at room temperature for 15 min, followed by 0.5% (w/v) Triton X-100 for 5 min. Primary antibody incubation was performed overnight at a 1:100 dilution, unless stated otherwise. Secondary antibody incubation was performed for 1 h at a 1:2,000 dilution. Detailed information on the antibodies used including their resources (company names, catalogue numbers) and dilutions are provided in the Reporting Summary.

Differentiation of hPSCs into intestinal spheroids or HLOs. All work using human pluripotent stem cells was approved by the University of Michigan Human Pluripotent Stem Cell Oversight Committee (HPSCRO). Stem cell lines are routinely monitored for chromosomal karyotype, pluripotency (using a panel of antibody and RT–qPCR markers), and for the ability to undergo multi-lineage differentiation. For intestinal spheroid generation, mycoplasma-free human ES cells (H9, NIH registry no. 0062) and iPS cells (line 20.1, source as previously described[13]) were cultured on Matrigel-coated plates and differentiated into intestinal tissue as previously described[13]. Floating spheroids present in the cultures on day 4 and day 5 of mid/hindgut induction were harvested for use in subsequent experiments. In some experiments, hESCs expressing a constitutively active H2BmCherry fluorescent reporter were used. This line was generated by infecting hESCs with a lentivirus containing PGK-H2BmCherry, which was a gift from M, Mercola (Addgene plasmid no. 21217) (ref. 37). For HLO generation, human ES cells (UM63-1, NIH registry no. 0277) were maintained, differentiated and expanded into HLOs as previously described[29].

Hydrogel formation and *in vitro* intestinal spheroid/HIO. To prepare PEG hydrogels, PEG-4MAL macromer (MW 22,000 or 44,000; Laysan Bio) was dissolved in 4-(2-hydroxyethyl)piperazine-1-ethanesulfonic acid (HEPES) buffer (20 mM in DPBS, pH 7.4). Adhesive and GPQ-W crosslinking peptides were custom synthesized by AAPPTec. Adhesive peptides RGD (GRGDSPC), AG73 (CGGRKRLQVQLSIRT), GFOGER (GYGGGP(GPP)$_5$GFOGER(GPP)$_5$GPC), IKVAV (CGGAASIKVAVSADR) and RDG (GRDGSPC) were dissolved in HEPES at 10.0 mM (5× final ligand density) and mixed with PEG-4MAL at a 2:1 PEG-4MAL/ligand ratio to generate functionalized PEG-4MAL precursor. Bis-cysteine crosslinking peptide GPQ-W (GCRDGPQG↓IWGQDRCG; ↓ denotes enzymatic cleavage site) or non-degradable crosslinking agent DTT (1,4-dithiothreitol; 3483-12-3, Sigma) was dissolved in HEPES at a density corresponding to 1:1 maleimide/cysteine ratio after accounting for maleimide groups reacted with adhesive peptide. For HIO encapsulation, spheroids were embedded and expanded in Matrigel for up to 30 days. Resulting HIOs were dislodged from the Matrigel and resuspended at 5× final density (final density: 2–4 HIOs per hydrogel) in intestine growth medium[38] and kept on ice. For human intestinal spheroid encapsulation, spheroids were harvested immediately after differentiation and were resuspended at 5× final density (final density: 20–30 spheroids per hydrogel) in intestine growth medium and kept on ice. For HLO encapsulation, the HLOs were dislodged from the Matrigel and resuspended at 5× final density (final density: 2–4 HLOs per hydrogel) in foregut growth medium[27,28] and kept on ice. To form hydrogels, adhesive peptide-functionalized PEG-4MAL macromer, cells and crosslinking peptide were polymerized for 20 min before addition of intestine growth medium. Matrigel-generated hPSC-derived HIOs were generated and cultured as described previously[13,38]. Passaging of HIOs cultured in PEG-4MAL hydrogels was performed similarly to tissue embedded in Matrigel, as previously described[27,38]. Briefly, HIOs were dislodged from the PEG-4MAL hydrogel, transferred to a sterile Petri dish, and manually cut into halves using a scalpel. HIO halves were resuspended at 5× final density (final density: 2–4 HIOs per hydrogel) in intestine growth medium[38] and mixed with hydrogel precursor solutions to form PEG-4MAL hydrogels. HIOs were passaged up to three times over the course of three weeks. Matrigel-generated HIOs were passaged as described previously[13,38]. Sample size was established as at least four hydrogels per condition with the premise that an outcome present in four different hydrogels under a specific condition will reveal the population behaviour submitted to this given condition.

A detailed protocol for generating the hydrogel and embedding HIOs can be found at the Protocol Exchange: http://dx.doi.org/10.1038/protex.2017.098.

Hydrogel characterization. The storage and loss moduli of hydrogels were assessed by dynamic oscillatory strain and frequency sweeps performed on a MCR 302 stress-controlled rheometer (Anton Paar) with a 9-mm-diameter, 2° cone, and plate geometry. Oscillatory frequency sweeps were used to examine the storage and loss moduli ($\omega = 0.5–100\,\mathrm{rad\,s^{-1}}$) at a strain of 2.3%.

Viability assay and quantification. PEG-4MAL gels were incubated in 2 μM Calcein-AM (live; Life Technologies), and 1 μM TOTO-3 iodide (dead; Life Technologies) in growth medium for 1 h. Samples were imaged using an Axiovert 35, Zeiss microscope. Quantification of viability was performed by calculating the percentage of the total projected area of a spheroid/organoid that stained positive for the live or dead stain using ImageJ (National Institute of Health, USA). The results are representative of three independent experiments performed with six PEG-4MAL/Matrigel gel samples per experimental group.

Inhibition of mediators of mechanotransduction. Inhibition of YAP, myosin II or Rho-associated kinase was performed using verteporfin (SML0534, Sigma), blebbistatin (203389, Calbiochem) and Y-27632 (688002, Calbiochem), respectively, by adding 10 or 30 μM to the intestine growth medium 20 min after spheroid encapsulation in hydrogel. Cell apoptosis/death was assessed 1 day after encapsulation using Annexin V/Dead Cell Apoptosis Kit (A13201, ThermoFisher). Samples were imaged using an Axiovert 35, Zeiss microscope. The results are representative of one experiment performed with 12 PEG-4MAL hydrogel samples per experimental group.

RT-qPCR. Total RNA from hESC day 0 spheroids or HIOs grown in PEG-4MAL hydrogels or Matrigel was extracted using the MagMax RNA isolation system and MagMax-96 total RNA isolation Kit (AM1830, ThermoFisher Scientific). cDNA was synthesized using the SuperScript VILO cDNA Synthesis Kit (11754-250, ThermoFisher Scientific). RT-qPCR was carried out using the QuantiTect SYBR Green PCR Kit (204145, Qiagen). Relative gene expression was plotted as arbitrary units using the formula: [2^ (housekeeping gene Ct − gene of interest Ct)] × 10,000. Primer sequences for RT-qPCR are provided in Supplementary Table 2.

Animal models. All animal studies were conducted following approved protocols established by University of Michigan's Institutional Animal Care and Use Committee (IACUC) in accordance with the US Department of Agriculture (USDA) Animal and Plant Health Inspection Service (APHIS) regulations and the National Institutes of Health (NIH) Office of Laboratory Animal Welfare (OLAW) regulations governing the use of vertebrate animals. Male (8 weeks old) NOD-scid IL2Rg-null (NSG) mice (Jackson Laboratory) were used for all experiments.

Kidney capsule implantation. Organoids were implanted under the kidney capsule of male NOD-scid IL2Rg-null (NSG) mice (Jackson Laboratory) as previously described[24]. Briefly, mice were anaesthetized using 2% isoflurane. The left flank was shaved and sterilized using chlorhexidine and isopropyl alcohol. A left-flank incision was used to expose the kidney. HIOs were manually placed in a subcapsular pocket of the kidney using forceps. An intraperitoneal flush of Zosyn (100 mg kg^{-1}; Pfizer) was administered prior to closure in two layers. The mice were euthanized and the transplant retrieved after 12 weeks. The results are representative of one experiment performed with three mice per condition (one organoid implanted per kidney capsule). Sample size was established as three with the premise that an outcome present in three different animals under a specific condition will reveal the population behaviour submitted to this given condition. No statistical method was used to predetermine sample size.

Colonic mucosal wound and HIO injections. NSG mice were anaesthetized by intraperitoneal injection of a ketamine (100 mg kg^{-1})/xylazine (10 mg kg^{-1}) solution. A high-resolution miniaturized colonoscope system equipped with biopsy forceps (Coloview Veterinary Endoscope, Karl Stortz) was used to biopsy-injure the colonic mucosa at 3–5 sites along the dorsal artery. Wound size averaged approximately 1 mm^2. HIO injection was performed on day 1 after wounding with the aid of a custom-made device comprising a 27-gauge needle (OD: 0.41 mm) connected to a small tube (Supplementary Fig. 6a). Endoscopic procedures were viewed with high-resolution (1,024 × 768 pixels) live video on a flat-panel colour monitor. The results are representative of two independent experiments performed with four mice per condition (five colonic wounds/injections per mouse) according to our previous experience with this model.

Wound closure quantification. Mice were anaesthetized by intraperitoneal injection of a ketamine (10 g l^{-1})/xylazine (8 g l^{-1}) solution (10 μl g^{-1} body weigh). To create mucosal injuries in the mouse colon and to monitor their regeneration, a high-resolution colonoscopy system was used. Each wound region was digitally photographed at day 1 and day 5, and wound areas were calculated using ImageJ (National Institute of Health, USA). In each experiment, three to four lesions per mouse were examined.

***In situ* hybridization (ISH).** ISH for mouse *Lgr5* expression was performed on frozen sections fixed with 4% paraformaldehyde. Slides were permeabilized with proteinase K (3115887001, Sigma-Aldrich) for 30 min at 37 °C, washed with Saline-Sodium Citrate buffer and then acetylated at room temperature for 10 min. A pre-hybridization step was performed for 1 h at 37 °C in a humidified chamber. A

DIG-labelled riboprobe diluted in hybridization buffer was incubated overnight at 68 °C. The slides were then washed and blocked for 1 h at room temperature followed by incubation with DIG antibody (11093274910, Sigma-Aldrich) overnight at 4 °C. The developer solution (11681451001, Roche) was incubated for 72 h until the *Lgr5*$^{+}$ cells became evident. ISH for *OLFM4* expression was performed using the RNAscope 2.5 HD manual assay with brown chromogenic detection (Advanced Cell Diagnostics) as per the manufacturer's instructions. The human 20-base-pair *OLFM4* probe was generated by Advanced Cell Diagnostics targeting 20 base pairs within 1111–2222 of *OLFM4* (gene accession NM_006418.4) and is commercially available. The results are representative of two independent experiments performed with four mice per condition (five colonic wounds/injections per mouse).

Statistics and reproducibility. All experiments were performed three or more times independently under similar conditions, except experiments shown in Fig. 6 and Supplementary Fig. 6, which were performed twice. Plots shown in Figs 1b,d, 3a–c and 6e, and Supplementary Figs 1c,d, 3 and 4 are for one of the experiments performed. Images shown in Figs 4 and 5, and Supplementary Fig. 5 were performed once. Images shown in Figs 2f,g, 3d,e, 4c,d, 5 and 6c,d, and Supplementary Figs 5b and 6b–d are representative of at least 20 tissue slices that were stained and imaged for each specific marker per experimental group for each independent experiment. Images shown in Figs 1a,c, 2a–e and 3a, and Supplementary Figs 2, 3 and 5a are representative of at least three images taken for each hydrogel per experimental group for each independent experiment. Images shown in Figs 4a,b and 6a,b,e are representative of images taken for all organoids/dissected kidneys or each individual wound/injection per mouse for each independent experiment. All statistical analyses were performed using GraphPad Prism 6.0. Statistical significance was calculated by one-way analysis of variance (ANOVA) with Tukey's multiple comparisons test (Figs 1b,d, 3a and 6e), two-way repeated measures ANOVA (Fig. 3b,c), and unpaired *t*-test with Welch's correction (Supplementary Figs 3b,c and 4) as described in the figure legends. *P* values of statistical significance are represented as $^{****}P < 0.0001$, $^{***}P < 0.001$, $^{**}P < 0.01$, $^{*}P < 0.05$.

Data availability. Source data for Figs 1b,d, 3a–c and 6e, and Supplementary Figs 1c,d, 3b,c and 4 have been provided in Supplementary Table 1. Additional images for data in Figs 4 and 5 are available at https://figshare.com/s/41e24da45c18e768536e. All other data supporting the findings of this study are available from the corresponding author on reasonable request.

37. Kita-Matsuo, H. *et al.* Lentiviral vectors and protocols for creation of stable hESC lines for fluorescent tracking and drug resistance selection of cardiomyocytes. *PLoS ONE* **4,** e5046 (2009).
38. Leslie, J. L. *et al.* Persistence and toxin production by *Clostridium difficile* within human intestinal organoids result in disruption of epithelial paracellular barrier function. *Infect. Immun.* **83,** 138–145 (2015).

nature cell biology

DOI: 10.1038/ncb3632

In the format provided by the authors and unedited.

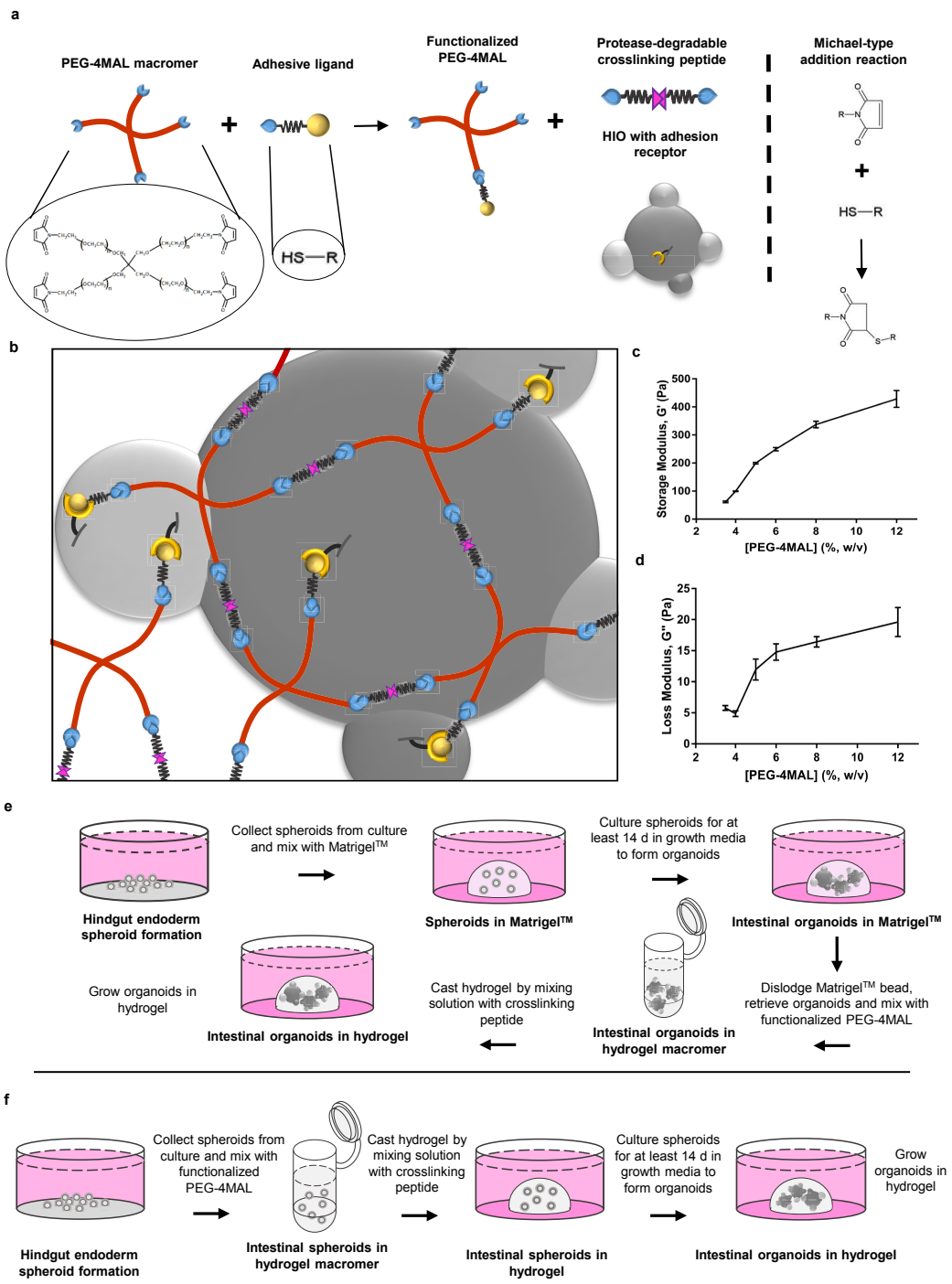

Supplementary Figure 1 PEG-4MAL hydrogel preparation and mechanical properties. (a) PEG-4MAL macromers are conjugated with thiol-containing adhesive peptide to produce a functionalized PEG-4MAL macromer, which is then crosslinked in the presence of HIOs/spheroids using protease-cleavable peptides containing terminal cysteines to form (b) hydrogel network. (c,d) Relationship between polymer density (wt%) and (c) storage modulus or (d) loss modulus (mean ± SEM; n = 10 independently prepared hydrogels per condition). (e) Schematic of spheroid development into HIOs within Matrigel™ and further growth within PEG-4MAL hydrogel. (f) Schematic of spheroid development into HIOs within hydrogel. Source data are available in Supplementary Table 1.

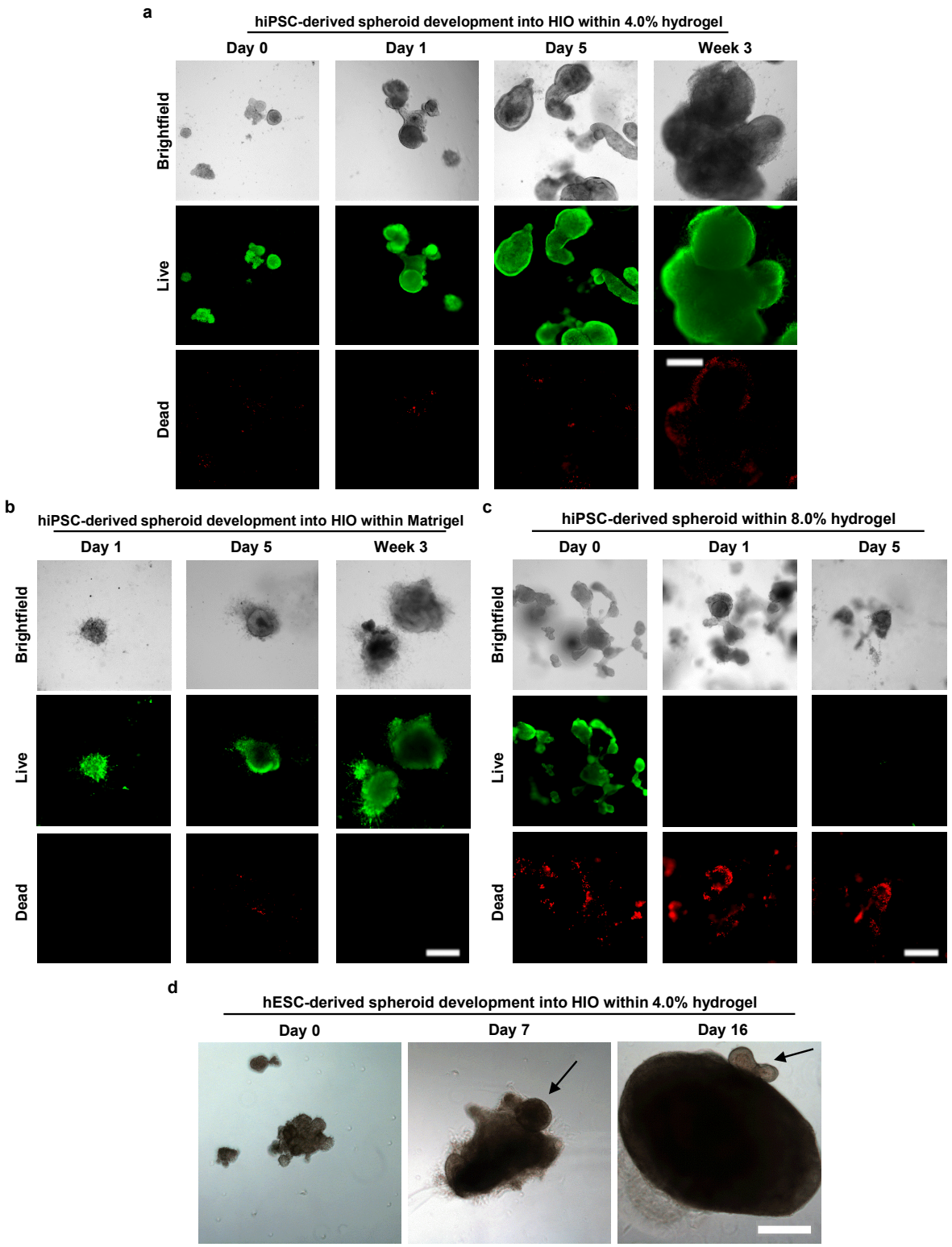

Supplementary Figure 2 PEG-4MAL hydrogel supports hiPSC-derived intestinal spheroid development into HIOs comparable to hESC-derived spheroids. Transmitted light and fluorescence microscopy images of hiPSC-derived HIO generation within (a) 4.0% PEG-4MAL hydrogels, (b) Matrigel^{TM}, or (c) 8.0% PEG-4MAL hydrogels. hiPSC-derived spheroid and HIO viability was assessed at different time-points after encapsulation. (d) Transmitted light microscopy images of hESC-derived HIO generation within 4.0% PEG-4MAL hydrogels. (a,c,d) These organoids were never encapsulated within Matrigel^{TM}. Black arrows show epithelial budding. Bar, 500 μm. Three independent experiments were performed and data is presented for one of the experiments. Every experiment was performed with 12 gel samples per experimental group (PEG-4MAL, Matrigel^{TM}).

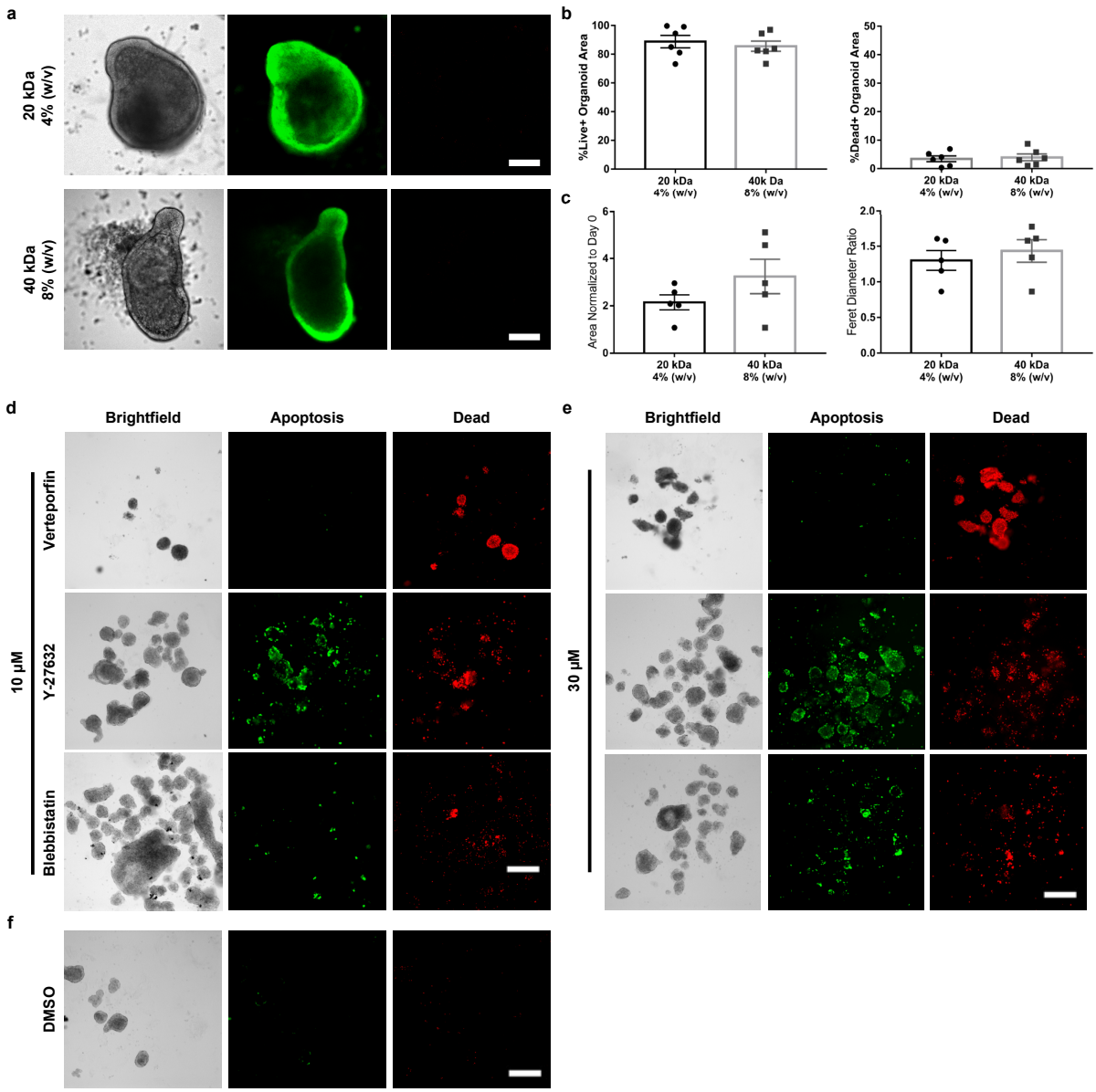

Supplementary Figure 3 PEG-4MAL hydrogels with different macromer sizes and mediators of mechanotransduction are essential for hESC-derived spheroid survival. (a) Transmitted light and fluorescence microscopy images of HIO generation within 20 kDa (4.0%) or 40 kDa (8.0%) PEG-4MAL hydrogels. HIO viability was assessed at 5 d after encapsulation. (b) Percentage of total organoid area stained for live or dead (mean ± SEM) after 5 d of encapsulation (n = 6 organoids analyzed per condition). (c) HIO projected area and Feret diameter normalized to Day 0 values (mean ± SEM) after 5 d of encapsulation (n = 5 organoids analyzed per condition). (b,c) Unpaired two-tailed t-test with Welch's correction showed no significant differences between HIO viability or HIO size parameters within 20 kDa (4.0%) and 40 kDa (8.0%) PEG-4MAL ($P > 0.05$). (d) Transmitted light and fluorescence microscopy images of spheroids cultured within 4.0% PEG-4MAL hydrogels supplemented with (d) 10 µM or (e) 30 µM of verteporfin, Y-27632 or blebbistatin, or (f) DMSO (vehicle control). Spheroids death was assessed by annexin-V (apoptosis) and propidium iodide (dead) labeling at 1 d after encapsulation. Bar, 100 µm. One experiment was performed with 12 PEG-4MAL hydrogel samples per experimental group. Source data are available in Supplementary Table 1.

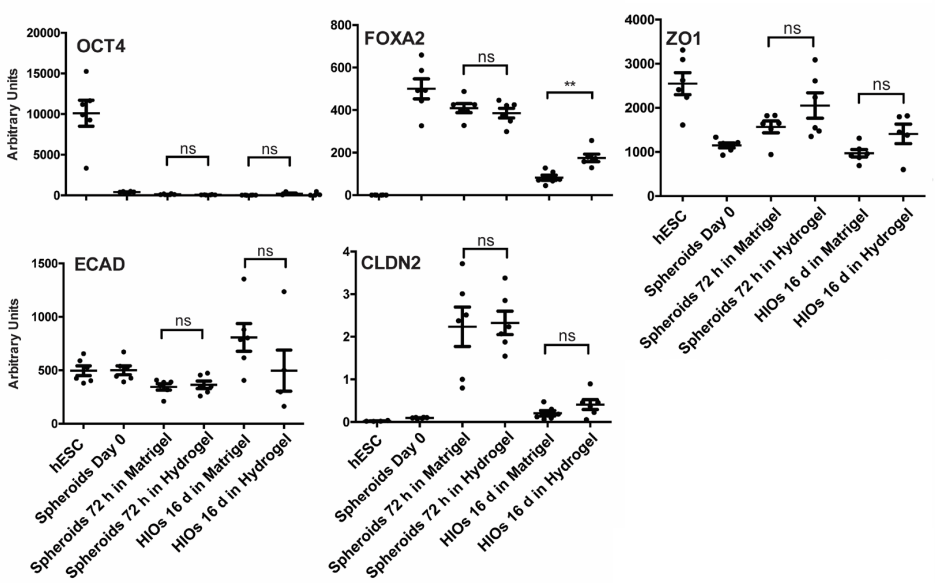

Supplementary Figure 4 Gene expression levels of PEG-4MAL-encapsulated spheroids are comparable to those embedded in Matrigel™. RNA levels of pluripotency (OCT4), endoderm (FOXA2), and epithelial junction (ZO1, ECAD and CLDN2) genes, as quantified by RT-qPCR (mean ± SEM; n = 6 samples per group). Unpaired two-tailed t-test was used to identify statistical differences between matrix types (**$P < 0.01$; ns, not significant). One experiment was performed. Source data are available in Supplementary Table 1. Primer sequences are provided in Supplementary Table 2.

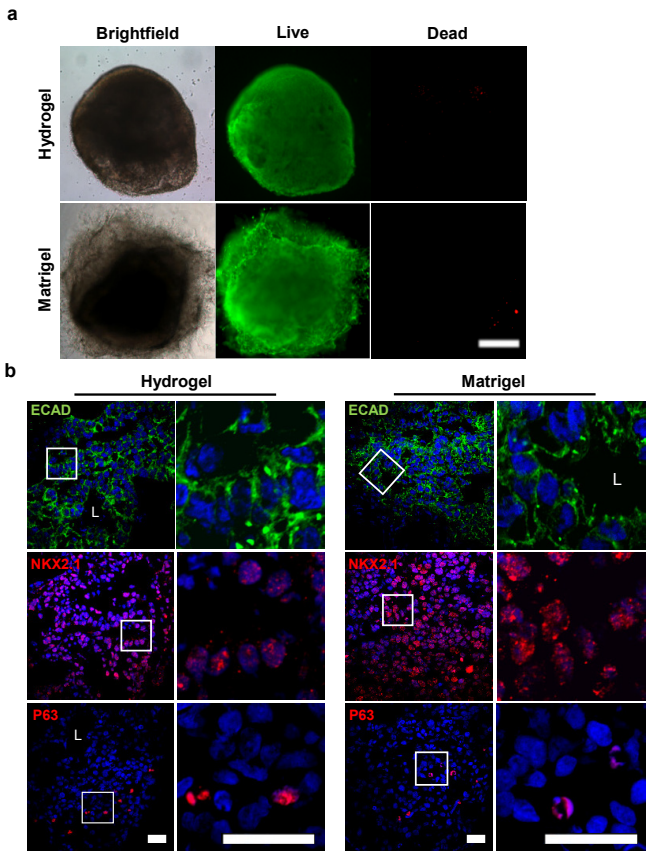

Supplementary Figure 5 PEG-4MAL hydrogel supports HLO development comparable to Matrigel™. (a) Transmitted light and fluorescence microscopy images of HLOs cultured in 4.0% PEG-4MAL hydrogels or Matrigel™. HLO viability was assessed at 7 d after encapsulation. Bar, 500 μm. (b) Fluorescence microscopy images of HLO at 7 d after encapsulation in 4.0% PEG-4MAL hydrogel or Matrigel™ and labeled for e-cadherin (ECAD), lung epithelia (NKX2.1), and basal cells (P63). DAPI, counterstain. "L" indicates HLO lumen. Bars, 25 μm. (a,b) One experiment was performed with 6 gel samples per experimental group (PEG-4MAL, Matrigel™).

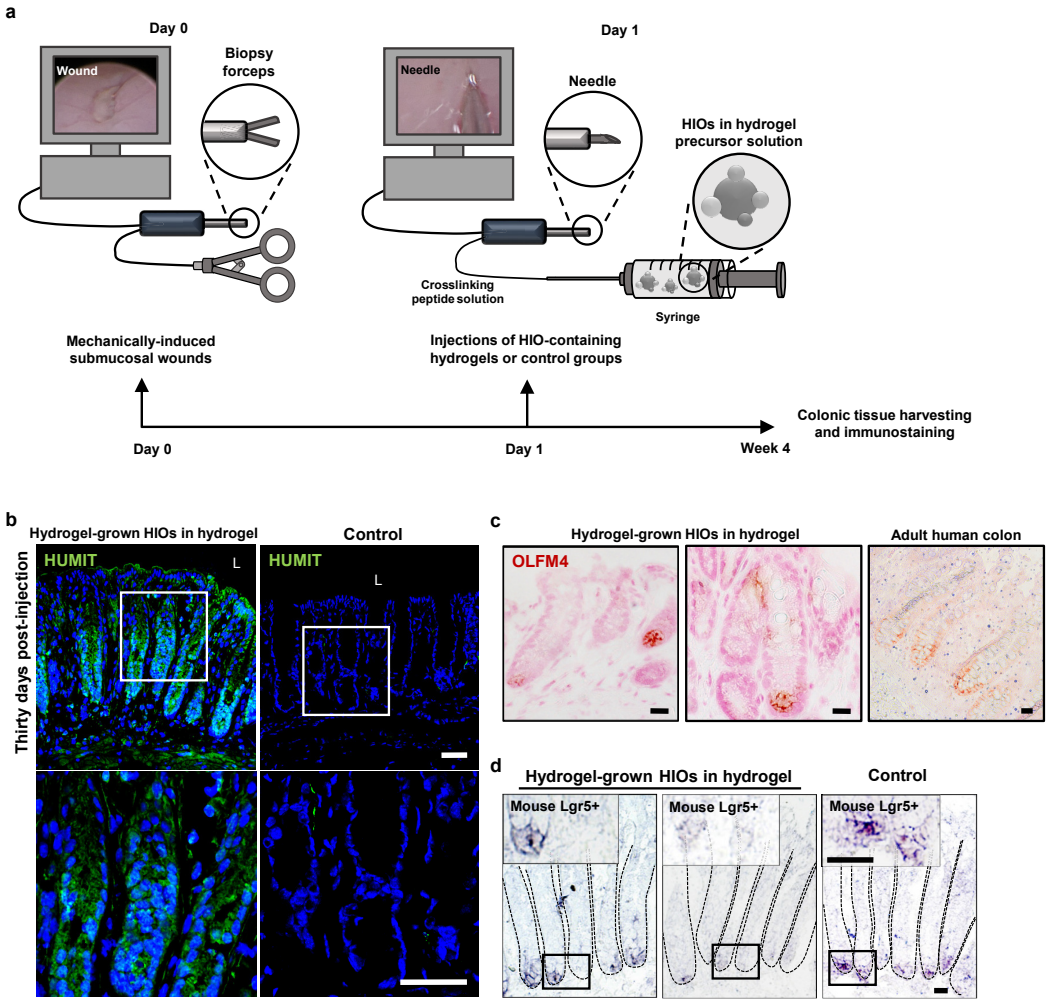

Supplementary Figure 6 PEG-4MAL hydrogel serves as an injectable delivery vehicle in colonic mucosal wound model and promotes HIO engraftment. (a) Mechanically-induced submucosal wounds were performed in the distal colon of mice using a mechanical probe through a mouse colonoscope. One day post-wounding HIOs generated in engineered 4% PEG-4MAL hydrogels or Matrigel™ were recovered from the matrix, mixed with the engineered hydrogel precursor solutions, and injected underneath the submucosal wounds. A group with no injections, HIOs injected in saline, or injection of HIO-free hydrogel precursor solutions were used as control groups. Distal colon tissue harvest, immunostaining and imaging was performed 4 weeks post-wounding. (b) Fluorescence microscopy images labeled for human mitochondria (HUMIT) of murine colonic tissue at the wound site at 4 weeks post-injection or control tissue. DAPI, counterstain. "L" indicates HIO lumen. Bar, 100 μm. (c) *In situ* hybridization images of (c) control adult human colon or sections taken at the mouse colonic wound site stained for human *OLFM4+* cells. (d) *In situ* hybridization images of tissue sections from mice colon that did not undergo colonic injuries or received HIO injections (control) and sections taken at the mouse colonic wound site stained for mouse *Lgr5+* intestinal stem cells. Bar, 50 μm. Two independent experiments were performed and data is presented for one of the experiments. Experiments performed with 4 mice per experimental group (five colonic wounds/injections per mouse; b-d).

Supplementary Table Legends

Supplementary Table 1 Statistics Source Data
Supplementary Table 2 Primer Sequences for RT-qPCR

nature research

Corresponding author(s): Jason R. Spence, Asma Nusrat and Andres J. Garcia

☐ Initial submission ☐ Revised version ☒ Final submission

Life Sciences Reporting Summary

Nature Research wishes to improve the reproducibility of the work that we publish. This form is intended for publication with all accepted life science papers and provides structure for consistency and transparency in reporting. Every life science submission will use this form; some list items might not apply to an individual manuscript, but all fields must be completed for clarity.

For further information on the points included in this form, see Reporting Life Sciences Research. For further information on Nature Research policies, including our data availability policy, see Authors & Referees and the Editorial Policy Checklist.

Experimental design

1. Sample size

   Describe how sample size was determined.

   No statistical method was used to predetermine sample size. For in vitro experiments, sample size was established as at least 4 hydrogels per condition (20-30 spheroids/hydrogel or 2-4 HIOs or HLOs/hydrogel) with the premise that an outcome present in all hydrogels under a specific condition will reveal the population behavior submitted to this given condition. For in vivo experiments, sample size was established as 3 with the premise that an outcome present in 3 different animals under a specific condition will reveal the population behavior submitted to this given condition.

2. Data exclusions

   Describe any data exclusions.

   The exclusion criteria was to exclude data from mice euthanized because of sickness. No animal was excluded from studies.

3. Replication

   Describe whether the experimental findings were reliably reproduced.

   All attempts at replication were successful.

4. Randomization

   Describe how samples/organisms/participants were allocated into experimental groups.

   For all experiments, one tube containing human intestinal spheroids, HIOs or HLOs was vortexed prior to mixing with different hydrogel precursor solutions, ensuring a random allocation of the biological tissue into the experimental groups. No randomization was used during inhibitor treatment or for animal experiments.

5. Blinding

   Describe whether the investigators were blinded to group allocation during data collection and/or analysis.

   Blinding was performed during outcome assessment. The researchers that performed the in vivo experiments were not the researchers that processed and analyzed the tissue resulting from these experiments.

Note: all studies involving animals and/or human research participants must disclose whether blinding and randomization were used.

6. Statistical parameters

For all figures and tables that use statistical methods, confirm that the following items are present in relevant figure legends (or in the Methods section if additional space is needed).

n/a	Confirmed
☐	☒ The exact sample size (*n*) for each experimental group/condition, given as a discrete number and unit of measurement (animals, litters, cultures, etc.)
☐	☒ A description of how samples were collected, noting whether measurements were taken from distinct samples or whether the same sample was measured repeatedly
☐	☒ A statement indicating how many times each experiment was replicated
☐	☒ The statistical test(s) used and whether they are one- or two-sided (note: only common tests should be described solely by name; more complex techniques should be described in the Methods section)
☐	☒ A description of any assumptions or corrections, such as an adjustment for multiple comparisons
☐	☒ The test results (e.g. *P* values) given as exact values whenever possible and with confidence intervals noted
☐	☒ A clear description of statistics including central tendency (e.g. median, mean) and variation (e.g. standard deviation, interquartile range)
☐	☒ Clearly defined error bars

See the web collection on statistics for biologists for further resources and guidance.

Software

Policy information about availability of computer code

7. Software

Describe the software used to analyze the data in this study.

Image acquisition of immunofluorescence experiments was performed using LAS X (Leica Microsystems, Inc.)
Quantification of spheroid/HIO viability and size parameters were performed using ImageJ 1.50b (National Institute of Health, USA).
RT-qPCR data analysis was performed using Microsoft Excel 2016 (Microsoft Corp.).
All statistical analyses were performed using GraphPad Prism 6.0.

For manuscripts utilizing custom algorithms or software that are central to the paper but not yet described in the published literature, software must be made available to editors and reviewers upon request. We strongly encourage code deposition in a community repository (e.g. GitHub). *Nature Methods* guidance for providing algorithms and software for publication provides further information on this topic.

Materials and reagents

Policy information about availability of materials

8. Materials availability

Indicate whether there are restrictions on availability of unique materials or if these materials are only available for distribution by a for-profit company.

No unique materials were used.

9. Antibodies

Describe the antibodies used and how they were validated for use in the system under study (i.e. assay and species).

The following antibodies were used according to the manufacturer's instructions. Primary antibody incubation was performed overnight at a 1:100 dilution, unless stated otherwise. Secondary antibody incubation was performed for 1 h at a 1:2000 dilution. Primary antibodies were validated for immunofluorescence labeling of frozen sections containing human or mouse tissue as specified in the manufacturer's website. Relevant citations can also be found in the manufacturer's website.
Primary Antibodies:
ZO-1 (33-9100, ThermoFisher Scientific)
β-CATENIN (610153, BD biosciences)
EZRIN (ab41672, Abcam) F(ab')2-Goat anti rabbit AlexaFluor 555 (A-21430, ThermoFisher Scientific)
KI67 (ab15580, Abcam)
CDX2 (MU392A-UC, Biogenex)
CHGA (sc-1488, Santa Cruz Biotechnology)
MUC2 (ab11197, Abcam)
DCAMKL-1 (DCLK1; ab31704, Abcam)
PDX1 (3470-1, Epitomics) Used at a 1:250 dilution
NUMA (MAB1281, EMD Millipore)
Human mitochondrial antigen, HUMIT (MAB1273, Millipore) Used at a 1:50 dilution
phalloidin-AlexaFluor 555 (A34055, ThermoFisher Scientific)
NKX2.1 (ab76013, Abcam)
P63 (sc-8344, Santa Cruz Biotechnology) Used at a 1:250 dilution.
E-cadherin, ECAD (610181, BD Biosciences) Used at a 1:500 dilution

Secondary Antibodies:
F(ab')2-Goat anti mouse AlexaFluor 488 (A-11017, ThermoFisher Scientific)
Goat anti rabbit AlexaFluor 488 (R37116, ThermoFisher Scientific)
Donkey anti rabbit Cy3 (711-165-152, Jackson Immuno)
Donkey anti-mouse AlexaFluor 488 (715-545-150, Jackson Immuno)

10. Eukaryotic cell lines

a. State the source of each eukaryotic cell line used.

Mycoplasma-free human ES cells (H9, NIH registry #0062).
iPS cells (line 20.1) were generated from normal human skin keratinocytes which were obtained from donors with informed consent (Cincinnati Children's Hospital Medical Center (CCHMC) Institutional Review Board protocol CR1_2008-0899) as described in Spence, 2011.
H2BmCherry-expressing human ES cell line was generated by infecting hESCs with a lentivirus containing PGK-H2BmCherry, which was a gift from Mark Mercola (Addgene plasmid # 21217).
HLOs were generated from human ES cells (UM63-1, NIH registry #0277).

b. Describe the method of cell line authentication used.

Stem cell lines are routinely monitored for chromosomal karyotype, at which time the number of chromosomes are confirmed, chromosomal abnormalities are ruled out and sex chromosomes of each line are confirmed. Functional and molecular authentication for pluripotency is assessed using a panel of antibody and qRT-PCR markers, and for the ability to undergo multi-lineage differentiation.

c. Report whether the cell lines were tested for mycoplasma contamination.

All cell lines tested negative for mycoplasma contamination.

d. If any of the cell lines used are listed in the database of commonly misidentified cell lines maintained by ICLAC, provide a scientific rationale for their use.

No cell lines used in this study were found in the database of commonly misidentified cell lines that is maintained by ICLAC and NCBI Biosample.

Animals and human research participants

Policy information about studies involving animals; when reporting animal research, follow the ARRIVE guidelines

11. Description of research animals

Provide details on animals and/or animal-derived materials used in the study.

Male (8 weeks old) NOD-scid IL2Rg-null (NSG) mice (Jackson Laboratory) were used for all our experiments.

Policy information about studies involving human research participants

12. Description of human research participants

Describe the covariate-relevant population characteristics of the human research participants.	The study did not involve human research participants.